sustainability

MDPI

Article

Sorption Efficiency of Potentially Toxic Elements onto Low-Cost Materials: Peat and Compost

Jacqueline Zanin Lima, Renan Marques Lupion, Isabela Monici Raimondi, Osni José Pejon and Valéria Guimarães Silvestre Rodrigues *

Department of Geotechnical Engineering, São Carlos School of Engineering, University of São Paulo (EESC-USP), 400 Trabalhador São Carlense Ave., São Carlos 13566-590, Brazil; jacqueline.zanin.lima@usp.br (J.Z.L.); renan.lupion@gmail.com (R.M.L.); isabela.monici@gmail.com (I.M.R.); pejon@sc.usp.br (O.J.P.)
* Correspondence: valguima@usp.br

Abstract: Anthropogenic activities can lead to elevated concentrations of potentially toxic elements (PTEs) in soil and water. Thus, the search for low-cost, ecofriendly and innovative sorbents is a global necessity. The present investigation addresses the performance of peat and compost derived from the organic fraction of municipal solid waste (OFMSW) as a sorbent of zinc (Zn), lead (Pb) and cadmium (Cd). The physicochemical features and effects of the initial concentration (equilibrium) and contact time (kinetic) were systematically analyzed by batch experiments. In addition, human bioaccessibility tests were conducted to compare the human health risk of these PTEs postsorption. The results showed that the sorption capacities followed the order: compost(Pb) > peat(Pb) > compost(Cd) > compost(Zn) > peat(Cd) > peat(Zn), indicating that compost had a better sorption potential. Kinetic data were well-fitted to the pseudo-first-order (PSO), pseudo-second-order (PFO), and Elovich equation models. The external diffusion model proposed by Mathews and Weber (M&W) indicated the contribution of diffusion as a sorption mechanism, mainly in the sorption of Zn, Pb and Cd onto compost and Pb onto peat. The bioaccessible fractions in the first stage (stomach conditions) were greater than those in the second phase (intestinal simulation). Pb has higher sorption capacities (10.511 and 7.778 mg g^{-1} for compost and peat, respectively) and lowers fraction bioaccessible (35 to 70%). These findings demonstrate that utilizing these low-cost sorbents seems promising for the remediation of PTE soils and contaminated waters. However, more experiments should be conducted, including desorption and multielement solutions, as well as field-tests to prove the long-term effects of application in large-scale and real conditions.

Keywords: cadmium; lead; zinc; organic fraction of municipal solid waste; batch experiments; human bioaccessibility; ecofriendly and innovative sorbents

Citation: Lima, J.Z.; Lupion, R.M.; Raimondi, I.M.; Pejon, O.J.; Rodrigues, V.G.S. Sorption Efficiency of Potentially Toxic Elements onto Low-Cost Materials: Peat and Compost. *Sustainability* **2021**, *13*, 12847. https://doi.org/10.3390/su132212847

Academic Editor: Dalia Štreimikienė

Received: 29 September 2021
Accepted: 29 October 2021
Published: 19 November 2021

1. Introduction

Soil is an integral system in dynamic balance with the environmental compartments of the hydrosphere, biosphere and atmosphere. It is considered a multicomponent and complex system because the different phases (gas, fluid, and solid phases) are formed by organic and inorganic compounds that interact among themselves. It is the environment where humans, animals, and plants live and extract most of their energy and food. Consequently, this system is certainly the ecosystem that accumulates the highest degree of anthropogenic stresses [1]. Since the industrial revolution, anthropic contaminant removal has been unable to keep pace with waste generation and population growth [2].

In this respect, soil exerts not only a drain function for contaminants but also a natural cap function to regulate the transport of the chemical elements. Soil cannot completely remove contaminating species. However, a balance related to the contaminant's binding to solid particles is observed [3]. Soil contamination usually occurs slowly. Nonetheless, in the long term, it may generate serious negative environmental impacts. It can be considered

the main cause responsible for the deterioration of groundwater because upon reaching the ground, contaminants that are not retained by the surface layers can penetrate and reach the groundwater, where they can spread, due to hydrodynamic dispersion, to increasingly distant sites [4].

Abandoned mining areas, mining waste-affected soils and acid mine drainage are common worldwide, and the environmental impact on soil and water is usually left unsolved. In these situations, especially in the case of metal ore mining, one of the most frequent problems is contamination by potentially toxic elements (PTEs) [5–11]. Other anthropogenic activities can also be sources of PTEs, especially when not carried out properly, including the disposal of industrial and urban waste, irrigation with wastewater, the application of mineral fertilizers to the soil, low-quality animal manure, pesticides, and sewage sludge [1,3].

The presence of PTEs (e.g., Zn, Pb, and Cd) interferes with the ecosystem functions provided by soil and with the normal metabolism of plants and animals, resulting in lethal physiological and neurological problems [12]. Zn is an essential nutrient; however, elevated Zn levels in humans by ingestion is dangerous for gastrointestinal and hematological systems [3,13,14]. Pb is a toxic element that has the potential to accumulate in humans. While human exposure can be determined by the Pb concentration in the blood, long-term exposure can be indicated by the presence of Pb in the bones [15,16]. Cd is carcinogenic, and exposure in humans causes damage to reproductive, hepatic, hematological and immunological functions. Oral exposure principally harms the kidneys and bones, and inhalation affects the kidneys and lungs [17,18].

There are several conventional recuperation technologies available for mine-impacted soil and water, and they are based on treatment and containment. Treatment technologies are based on the modifying of the contaminant composition or limiting its mobility, and they include chemical treatment, stabilization, solidification, solvent extraction, and soil flushing. When these technologies cannot mitigate contaminants to an acceptable condition, diversion and containment technologies are utilized. These processes involve landfill disposal, application of several cutoff walls, pumping groundwater for treatment, capping, and erosion control [19]. Some of these treatment processes for PTE contamination (e.g., permeable reactive barriers and sealant barriers) include sorption. Research on PTE sorption has focused on the use of low-cost and effective sorbents. Previous studies have shown that a variety of organic materials can be used for this purpose, such as sawdust from deciduous trees [20], coffee husks [21], *Luffa cylindrica* sponge [22], tea waste [23], sugarcane waste [24,25], corn cob and eggshell [26], and biochars [27–30]. The aim of the present study is to evaluate the sorption of PTE by tropical peat and compost derived from the organic fraction of municipal solid waste (OFMSW). Tropical peat was selected because it is one of the most traditional sorbents, although knowledge of tropical peatlands is still lacking, while OFMSW was selected to find alternative innovative uses with regard to organic municipal waste management.

Peat is one of the most promising materials for building cover barriers [31], and its use for improving a soil as an environmental protection barrier has already been confirmed [32]. Peat is a reactive material that is suitable as a natural sorbent [33]. Many studies of peat from temperate and boreal climate zones have confirmed its high sorption capacity for PTE. Studies on peat have focused on its use in wastewater treatment [34–36], leachate [37], agricultural areas [38], soil contamination [39,40], as a phytostabilizing agent for mine tailings [41], its reactive permeable barrier [42], its industrial waste landfill hydraulic barrier layers [43], and efforts to quantify its effects on atmospheric pollution [44].

However, peat is a nonrenewable natural resource that requires a long period for humification and the coating of a landfill generally consumes large quantities of materials to meet the technical requirements and capacity of immobilizing contaminants. In this respect, some studies have been conducted to analyze the characteristics of possible alternatives, such as composts resulting from composting [45], thus following the principles of a circular economy and contributing to completing the waste management cycle [46]. At the

global level, OFMSW corresponds to the largest portion of municipal solid waste (MSW) (46%) [47]. Due to the ease, simplicity, and efficiency of implementing composting, it is a viable alternative for municipal management of organic waste, principally in developing countries [48]) (such as Brazil). Compost is a reactive material with a PTE sorption capacity that has been previously demonstrated, and studies have positively evaluated its use in the treatment of industrial wastewater [49] and contaminated soils and water [40,50–56].

In humid tropical regions, such as Brazil, most soils are acidic and commonly present low organic matter [57]. However, compost is usually close to neutral, with pH values varying between 7.0 and 8.5 [1,58]. For most PTEs, alkaline conditions favor their immobilization [3,59]. Therefore, PTE-contaminated acidic soils may benefit from the application of alkaline materials, such as compost, which could offer strategic and cost-effective advantages. Furthermore, while peat is found only in specific regions, compost derived from OFMSW can be produced in a local community next to the contaminated site and is a highly sustainable technology [60].

The specific contamination impact depends on the PTE in question and its availability, which is associated with its mobility in the ecosystem [12]. Unlike pedogenic inputs, PTEs derived from anthropogenic activities generally present high bioavailability [1,61]. In general, the contaminants present in the soil solution are the most bioavailable since organisms, plants and other species have direct access to absorption via this fraction [62]. However, to determine the real impact of this mobility on the biota, it is necessary to study its bioaccessibility. Concerning the risk assessment for human health, the main route of exposure to a contaminant is oral intake [63]. Thus, it is necessary to use a practical methodology to measure the fraction of the contaminant in the soil that can enter the blood system and cause toxic effects [64]. For the evaluation of this risk, extractions were developed to imitate mammalian digestive processes and measure the human bioaccessibility of a contaminant bound to a solid phase [65].

For mining wastes, Ruby et al. [66] indicate that these in vitro methods may represent an effective tool in geochemical and physiological evaluations for the control of PTE accessibility to the human body. Thus, PTE bioaccessibility is widely used in the assessment of mining waste-contaminated soils, including abandoned mining and smelter sites [9,67–70]. Conversely, limited research has focused on whether performing soil organic amendments by increasing the organic carbon provides significant protection against PTE sorption for exposed individuals [71–73]. In addition, few studies in the literature have presented the results of PTE bioaccessibility in sorbents, such as peat and compost.

The purpose of the present study was to investigate the feasibility of using peat and compost for the removal of PTE. For this reason, physicochemical characterization and sorption experiments (equilibrium and kinetics) were conducted using Zn, Pb, and Cd as sorbates. The tropical peat was collected in the Mogi-Guaçu River Basin (São Paulo State, Brazil), while the compost was derived from the OFMSW. In addition, human bioaccessibility experiments were also performed to compare the human health risk of these PTEs once in a bioaccessible form. This analysis is necessary to evaluate PTE behavior after the reactive medium (such as peat or compost) is discarded in the environment (after saturation). Knowledge of the peat and compost retention capacity as well as the potential bioaccessibility of metals (particularly the notorious PTE pollutants Zn, Pb and Cd) will provide additional insights into the potential threats to human health and the environment for investigations on how to protect and recover contaminated mining sites with these organic materials.

2. Materials and Methods

2.1. Sample Preparation

The compost was generated by a composting process at mid-scale and under environmental conditions from the OFMSW of the restaurant of the São Carlos School of Engineering, University of São Paulo (São Carlos, Brazil), via the windrow composting

method, as previously described [54]. The peat was collected in a commercial peat extraction zone in Cravinhos City (Mogi-Guaçu River Basin in São Paulo State, Brazil).

2.2. Compost and Peat Characterization

The pH (in $CaCl_2$) was measured after contact material with $CaCl_2$ (0.01 mol L^{-1}) with a ratio of 1:5 (w:v) [74]. The pH (in H_2O), potential redox (Eh) and electrical conductivity (EC) were determined according to the method adapted from EMBRAPA [75] using a ratio of 1:2.5 (w:v) in deionized water. The total moisture content occurred in two steps: (i) oven drying samples at 60–65 °C for 24 h and (ii) subsequent drying at 110 °C [76]. The water retention capacity (WRC) for the lower tension (1 kPa) was based on Brasil [77]. The cation exchange capacity (CEC) was performed by the titration method [74]. The organic matter content and total mineral residue were carried out in a furnace by loss-on-ignition at 550 °C [76,78]. The elemental analysis followed the methodology of Brasil [74]. Specifically, the C content was determined by oxidation with dichromate followed by titration; the N concentration was determined by sulfuric digestion (Raney's method); the P content was determined by extraction using hydrochloric acid and then the molybdovanadophosphoric acid spectrophotometric method; the K content was determined by extraction using hydrochloric acid and then quantification by the flame photometry method (Digimed DM 32 Flame Photometer); the S content was determined using the gravimetric barium sulfate method; and the Ca and Mg contents were determined by extraction with hydrochloric acid and then the atomic absorption spectrometry method (PerkinElmer Model 1100B Atomic Absorption Spectrophotometer). The Cd, Pb and Zn concentrations were determined by inductively coupled plasma optical emission spectrometry (ICP-OES Horiba Jobin Yvon, Ultima 2 model, with radial vision and sequential scanning system). X-ray fluorescence (XRF) was determined in an X-ray fluorescence spectrometer (Axios Advantage, Panalytical).

Scanning electron microscopy (SEM) and X-ray energy dispersive spectroscopy (EDS) were performed with the samples placed in stubs and coated with 6 nm of carbon. The photomicrographs were obtained in a ZEISS LEO 440 Electronic Microscope (Cambridge, England) with an OXFORD detector (Model 7060), which was operated with a 20 kV electron beam and a current of 2.82 A. The EDX Link Analytical Equipment (Isis System Series 300) allowed for the analysis of EDS with a SiLi Pentafet detector and ATW II (Atmosphere Thin Window), with a resolution of 133 eV at 5.9 keV and an area of 10 mm^2.

The specific surface area (SSA), total pore volume (V_p) and average pore radius (R_p) were determined by nitrogen physisorption, with the sorption and desorption isotherms acquired in a Quantachrome NOVA 1000 version 10.02 instrument using the Brunauer-Emmett-Teller (BET) method and the Barrett-Joyner-Halenda (BJH) method. Samples were initially degassed at 200 °C under a N_2 flow for 6 h.

The Fourier transform infrared fluorescence (FTIR) assays were performed in a Fourier transform infrared spectrophotometer (IRAffinity 1, Shimadzu) using the direct sample transmission method with dilution in potassium bromide (KBr). Spectra were acquired in the 4000 to 400 cm^{-1}, with a resolution of 4 cm^{-1} and 32 cumulative sweeps.

2.3. Sorption Equilibrium Studies

The procedures for carrying out the PTE sorption equilibrium experiment were based on and adapted to the methodology used by ASTM D4646 [79]. Peat and compost samples with a particle size < 2 mm were previously oven-dried for 48 h at 50 °C. Common potentially toxic elements in metal ore mining waste were selected for analysis: Zn, Pb and Cd. The batch equilibrium test was conducted in triplicate in Falcon tubes using a ratio of 1:50 (w:v), with 1 g of material (peat or compost) and 50 mL of a single synthetic solution with PTE concentrations up to 220 mg L^{-1} using $ZnCl_2$, $PbCl_2$ and $CdCl_2$ H_2O. This ratio was chosen according to previous tests using ratios of 1:5, 1:10, 1:50, 1:80 and 1:100 [80]. The concentration limits are consistent with the characteristic values of mining waste [5,6,8]. The experiments were maintained under the same stable room temperature (close to 25 °C) and 10 to 20% mechanical stirring. After 24 h of contact [79], the samples

were centrifuged and filtered on filter paper (with a weight of 80 g m^{-2} and particle retention of 4–12 µm). Afterward, the filtrates were analyzed in a PinAAcle 900F Atomic Absorption Spectrophotometer (PerkinElmer). The initial and final values of pH and Eh were measured for all samples.

With the results, it was possible to calculate the sorbed concentration or the removal capacity after equilibrium q_e (mg g^{-1}) with Equation (1):

$$q_e = \frac{[V_{solution}\ (C_0 - C_e)]}{M_{reactive\ material}} \quad (1)$$

The respective removal percentage R (%) could be calculated using Equation (2):

$$R = \left[\frac{C_0 - C_e}{C_0}\right] \times 100 \quad (2)$$

where $V_{solution}$ is the volume of solution (L); C_0 and C_e are the initial concentrations and equilibrium concentrations (mg L^{-1}), respectively; and $M_{\ reactive\ material}$ is the exact mass of the reactive material sample (g).

2.4. Sorption Kinetic Studies

Determining the sorption kinetics are important for understanding the metallic ion removal process using sorbents. Thus, the data can be well understood by examining kinetic models and determining the rate-controlling mechanism. Kinetic batch experiments were conducted based on and adapted to the methodology used by [81]. This test was initiated in duplicate using a similar ratio of equilibrium experiments (1:50), but mixing 5 g of solid material (peat or compost) with 250 mL of a single solution with a PTE concentration of 220 mg L^{-1} (solid:solution ratio of 1:50). The mixtures were maintained under the same stable room temperature (close to 25 °C) and 10 to 20% mechanical stirring. After each time interval (0, 15, 30, 60, 90, 120, 150, 180, 210, 240, 480, and 1440 min), an aliquot of the suspension was collected and filtered and the filtrate was analyzed for the remaining PTE concentrations using a PinAAcle 900F Atomic Absorption Spectrophotometer (PerkinElmer).

The experimental kinetics data were fitted to pseudo-first-order (PFO), pseudo-second-order (PSO), Elovich, Mathews and Weber (M&W), and Weber and Morris (W&M) models using the "user interface" (UI) from Microsoft Excel software, as developed by [82]. To support the best fitting of the models to the experimental data, the statistical parameter coefficient of variation (R^2) (Equation (3) and analysis and residual sum of squares error (SSE) (Equation (4)) were performed.

$$R^2 = \frac{\sum(q_{mean} - q_{cal})^2}{\sum(q_{cal} - q_{mean})^2 - \sum(q_{cal} - q_{exp})^2} \quad (3)$$

$$SSE = \sum(q_{exp} - q_{cal})^2 \quad (4)$$

2.4.1. Pseudo-First-Order (PFO)

This model is a simple kinetic analysis of sorption. Also known as the Lagergren equation, it was the first velocity equation created to characterize the sorption of a liquid/solid system based on the solid capacity [83]. The basic assumptions of the PFO model are (i) a high initial concentration of sorbate, (ii) applicable to the initial stage of sorption, and (iii) a few active sites exist in the sorbent surface; that is, sorption is not controlled by sorption in the active sites [82]. To obtain an equation with experimental data, an equilibrium sorption capacity (q_e) must be known. However, as the process is extremely slow, the alternative is an extrapolation of the experimental data to an infinite time or use of a trial-and-error method [83]. This model generally does not fit well for the whole range of contact times and is normally applicable only at the initial stage of the sorption process.

The pseudo-first-order kinetic model is generally expressed as follows (Equation (5)) [84]:

$$\frac{dq_t}{dt} = k_1(q_e - q_t) \quad (5)$$

The model after integration with the initial conditions of $q_0 = 0$ is presented as Equation (6):

$$q_t = q_e\left(1 - e^{-k_1\ t}\right) \quad (6)$$

where q_t and q_e (mg g^{-1}) denote the sorption capacities at time t and equilibrium (min), respectively, and k_1 is the rate constant of first-order sorption (min^{-1}).

2.4.2. Pseudo-Second-Order (PSO)

This kinetic model assumes that the sorption capacity is proportional to the number of occupied active sites present in the sorbent [84]. The PSO model could represent three conditions: (i) the initial concentration value is low, (ii) applicable in the final phase of sorption and (iii) the sorbent is abundant in active locations [82]. It was used for the first time to model Pb sorption in peat [85]. This model has been largely applied to the sorption of contaminants from aqueous solutions to describe various sorption processes [82,86]. The PSO model based on the sorption equilibrium capacity may be expressed by a differential equation (Equation (7) [87] and the integrated form [82] (Equation (8)):

$$\frac{dq_t}{dt} = k_2\ (q_e - q_t)^2 \quad (7)$$

$$q_t = \frac{q_e^2\ k_2\ t}{1 + q_e\ k_2\ t} \quad (8)$$

where k_2 represents the pseudo second-order rate constant (mg g^{-1} min^{-1}). This rate may be directly dependent on the sorbed PTE ion concentrations.

According to theoretical analysis [88], the rate constant is a linear function of the initial concentration of solute for systems whose sorption kinetics obey the PFO model. Nonetheless, the rate constant is a complex function of the initial concentration of solute for systems that obey the PSO model.

2.4.3. Elovich Kinetic Model

Another model for the analysis of sorption kinetics is the Elovich model. This equation is an empirical model that considers the surface of the heterogeneous sorbent as well as the increase in activation energy as the sorption time advances [82]. It was developed to describe the chemical sorption present in a gas-solid system. However, it has also been used to adequately describe sorption kinetics in liquid-solid systems [81,86,87,89–91]. This model assumes that the solid surfaces are energetically heterogeneous and that the kinetics of sorption cannot be affected by desorption or interactions between the sorbed species [92].

The Elovich kinetic model is commonly represented by Equation (9) [93], and integrating this equation for the condition of $q_o = 0$ generates Equation (10) [82]:

$$\frac{dq_t}{dt} = \alpha\ e^{-\beta\ q_t} \quad (9)$$

$$q_t = \frac{1}{\beta}\ln(1 + \alpha\ \beta\ t) \quad (10)$$

where α is the initial sorption rate (mg g^{-1} min^{-1}) and β is the desorption constant (mg g^{-1}) during any one experiment.

2.4.4. Mathews and Weber (M&W)

There are stages in the sorption process by porous sorbents. First, the sorbate is transferred from the aqueous solution to the external bordering of the sorbent (film diffusion). Then, the particles enter particular active sites (particle diffusion). Finally, sorption interactions occur on the interior of the porous sorbent [94].

The previous models are not able to identify the diffusion mechanisms. The possibility of the diffusion of sorbate in a bounding liquid film around the sorbent is the slowest step and was assumed by several external diffusion equations, such as the Mathews and Weber model presented in Equation (11) [95]:

$$q_t = \frac{C_0}{m_s}\left(1 - e^{-k_{M\&W}\ S\ t}\right) \tag{11}$$

where m_s denotes the mass of sorbent per unit volume of solution (g L^{-1}) and $k_{M\&W}\ S$ describes the external diffusion (cm min^{-1} cm^{-1}).

2.4.5. Weber and Morris (W&M)

The W&M model is one of the most commonly used models to describe the intraparticle diffusion, and it is described as follows (Equation (12)) [96]:

$$q_t = k_{W\&M}\ t^{1/2} \tag{12}$$

where k_{id} is the intraparticle diffusion rate constant (mg g^{-1} $min^{-1/2}$).

A plot of the square root of time ($t^{1/2}$) against q_t fits a linear relationship if intraparticle diffusion is implied in the sorption process. The plot that passes through the origin suggests that intraparticle diffusion is the rate-controlling step. If the linear relationship does not pass through the origin, then intraparticle diffusion is not the only rate-limiting step, and other kinetic models may simultaneously control sorption [82,96]. The Weber and Morris model represents a simplistic approximation of the pore diffusion kinetics without accounting for the effects of the pore dimensions. The effect of pore diffusion processes on the uptake of potentially toxic elements needs to be studied in more detail, including the impacts of pore radius and size on the sorption kinetics [92].

2.5. Bioaccessibility Test

The PTE bioaccessibility for humans in the peat and compost postsorption equilibrium was analyzed using a modification of the in vitro physiologically based extraction test (PBET) [97] at a 1:100 solid:liquid ratio [98]. The extraction occurred sequentially in two stages in a dry bath incubator/block heater equipment, and it was performed in duplicate.

(i) To simulate the gastric phase (first phase): 50 mL of 0.4 M glycine solution adjusted to pH 1.5 with HCl was added to 0.5 g of dry peat. The solution was maintained at 37 °C and stirred occasionally for 1 h, and then an aliquot of the supernatant (10 mL) was sampled and filtered;

(ii) To simulate passage from the gastric to the intestinal phase (second phase): the pH of the remaining extract was elevated using $NaHCO_3$; the solid-solution ratio (1:100) was maintained constant by adding glycine; the suspension was maintained at 37 °C and stirred occasionally for 3 h; and an aliquot of the supernatant was sampled and filtered (filter paper similar to the first phase).

The PTE dissolved in the filtrates was analyzed in a PinAAcle 900F Atomic Absorption Spectrophotometer (PerkinElmer).

3. Results

3.1. Compost and Peat Properties

The physicochemical characteristics of the peat and compost used in the experiments are listed in Table 1. The compost pH was higher than the peat pH (Table 1), and the values

were within the expected range for these materials. For each material, the pH in water was higher than the pH in $CaCl_2$ due to the so-called salt effect. During composting, numerous chemical and biological reactions occur that regulate the acidic conditions and result in the generation of a final product with a pH in the range of 7.0 to 8.5 [99]. The studied compost had a slightly basic pH in water (7.4, Table 1) and may be an indication of its maturity. In contrast, peat commonly has a pH ranging from 3.0 to 6.0, with higher values associated with a lower decomposition level [100]. This peat acidic character is associated with humic substances related to the COOH and OH group ionization present predominantly in its structure. Dick et al. [101] indicated that at pH values from 4.0 to 5.0, most of the carboxylic functional groups are already dissociated, thus contributing positively to cation exchange. The peat evaluated in this study with a pH in water of 5.0 could be classified as moderately acidic (pH in the range of 4.5 to 5.5) [102].

Table 1. Physicochemical properties of compost and peat.

Parameter	Compost	Peat
pH: $CaCl_2$ 0.01 M	5.4	3.9
pH: H_2O	7.4	5.0
Eh (mV)	+268	+432
EC ($\mu S\ cm^{-1}$)	665	448
Moisture: 65 °C (%)	36.78	7.99
Moisture: 110 °C (%)	1.52	2.29
Total Moisture (%)	38.30	10.28
WRC (%)	65.26	36.28
CEC ($mmol_c\ kg^{-1}$)	340.00 [b]	910.00 [c]
OM [a] ($g\ kg^{-1}$)	186.60	447.60
IMR [a] ($g\ kg^{-1}$)	695.30	417.60
SMR [a] ($g\ kg^{-1}$)	94.00	110.50
TMR [a] ($g\ kg^{-1}$)	789.30	527.60
C [a] (%)	8.32	23.36
N[a] (%)	0.82	1.26
C/N	10	19
P [a] ($g\ kg^{-1}$)	2.01 [b]	0.66
K [a] ($g\ kg^{-1}$)	1.58 [b]	0.58
Ca [a] ($g\ kg^{-1}$)	28.60 [b]	1.80
Mg [a] ($g\ kg^{-1}$)	1.30 [b]	1.10
S [a] ($g\ kg^{-1}$)	0.30 [b]	0.80
Cd [a] ($mg\ kg^{-1}$)	<5	<5
Pb [a] ($mg\ kg^{-1}$)	24.50	<5
Zn [a] ($mg\ kg^{-1}$)	57.50	<5
XRF	SiO_2 (44.5%); Al_2O_3 (11.0%); Fe_2O_3 (5.8%); CaO (1.6%)	SiO_2 (33.9%); Al_2O_3 (12.3%); Fe_2O_3 (2.2%); TiO_2 (2.0%)

[a]: The parameters are presented on a dry basis (65 °C); [b]: from [54]; [c]: from [80]. Eh: potential redox; EC: electrical conductivity; WRC: water retention capacity; CEC: cation exchange capacity; OM: organic matter; IMR: insoluble mineral residue; SMR: soluble mineral residue; TMR: total mineral residue; XRF: X-ray fluorescence.

Compost and peat revealed oxidizing conditions with redox potential values of +268 and +432 mV, respectively. Regarding moisture, the compost exhibited higher total values, and most of this retained water could be lost at 65 °C. The water retention capacity of the compost was also higher than that of peat (65.26 and 36.28%, respectively). The peat presented a larger organic matter portion than the compost (447.60 and 186.60 g kg^{-1}, respectively). Consequently, the mineral residue fraction (TMR) in the peat was lower than that in the compost (527.60 and 789.30 g kg^{-1}, respectively). As organic matter contributes positively to the increase in CEC [103], peat exhibited a higher CEC than compost (910.00 and 340.00 $mmol_c\ kg^{-1}$, respectively). Meanwhile, the compost showed a larger insoluble mineral residue portion, silica and electrical conductivity than peat (Table 1). As expected,

peat had a higher organic carbon content than compost (23.36 and 8.32%, respectively) and a higher C/N ratio. The C/N ratio for the compost was 10; thus, it was classified as a material in a decomposed and stable state according to Kiehl [76].

Regarding the target PTEs (Zn, Pb and Cd), peat and compost presented concentrations below the respective values of prevention (86, 72 and 1.3 mg kg^{-1}), thus indicating that the introduction of these materials in the soil does not inhibit the functionality of the natural environment (Guiding Values for Soils) [104]. In addition, data from the literature highlighted the need for special care to avoid the incorporation of large concentrations of PTEs in the final products. The composts studied by Farrell and Jones [50] and Venegas et al. [105] presented mean Pb concentrations of 906 and 89 mg kg^{-1} and Zn concentrations of 505 and 523 mg kg^{-1}, respectively. Depending on the situation, these values may even make it impossible to use these sorbents for the actual remediation of a contaminated area. Thus, it is important to be careful in obtaining and transporting the feedstock material, such as by segregation at the source, as in this study, which yielded good results.

The results shown in Table 1 are generally within the range of the expected values for these material typologies. In comparison, studies with MSW-derived composts revealed pH_{H2O} values in the range between 7.0 and 8.5 [50,105,106]. Smaller values (5.4 to 6.7) were presented by Simantiraki et al. [106] for materials with shorter maturation times. The composts commonly have different CECs of 789.55 and 1050.00 $mmol_c$ kg^{-1} for organic matter contents of 835.70 and 560.00 g kg^{-1}, respectively [105,107]. Faverial et al. [108] concluded that the characteristics of compost are strongly influenced by climatic conditions during composting: the composts produced in a tropical climate (high temperature and precipitation) exhibited greater losses of C and nutrients, thus contributing to less organic matter and nutrient content in relation to composts produced in temperate climate regions. For example, studies carried out on European composts (temperate climate) described C contents of 24.60 and 27.00% [51,105], which are much higher than those found in this study for a tropical compost.

In studies characterizing Brazilian peats collected in the Mogi-Guaçu River basin but in different municipalities, Raimondi et al. [80] found a pH_{H2O} value of 5.9, an OM of 510.60 g kg^{-1}, and a CEC of 1160.00 $mmol_c$ kg^{-1} and Crescêncio Junior [42] found a pH_{H20} of 4.3, an organic matter content of 682.00 g kg^{-1}, and CEC of 710.00 $mmol_c$ kg^{-1}. Other Brazilian peats had CECs of 670.00, 1355.00, and 1819.00 $mmol_c$ kg^{-1} for organic matter contents of 325, 734, and 971 g kg^{-1}, respectively [42,109]. For peat from temperate regions (Turkey and Sweden), Gündoğan et al. [110] and Kalmykova et al. [37] obtained CECs of 971.00 and 309.00 $mmol_c$ kg^{-1}, respectively. The organic matter content of peat is variable, with peat analyzed by Kiehl [76] presenting variable OM content between 305 and 952 g kg^{-1}. The C content is directly associated with the organic portion, and the percentage of the elemental composition varies, with C fluctuating from 12.0 to 60.0% and for N varying from 0.3 to 4.0%. Batista et al. [111] analyzed three Brazilian peats and found that one of them exhibited a carbon content of 53.10%, which was much higher than that of the others (6.23 and 5.12%).

Scanning electron micrographs indicated differences in surface morphology between compost and peat. Both sorbents showed clear granulometric variations, but the compost grains were relatively larger and more heterogeneous compared to peat. This can be clearly seen in Figure 1, where both materials are depicted on the same scale.

Although the peat grains exhibited greater sphericity, the compost was formed by particles of different shapes (spherical to elongated), including some that resembled compostable materials that are more difficult to degrade (such as sawdust) (Figures 1 and 2). The compost exhibited an irregular structure, with some smoother particles and rougher particles, which can contribute to greater porosity in relation to peat (Figure 2A,B).

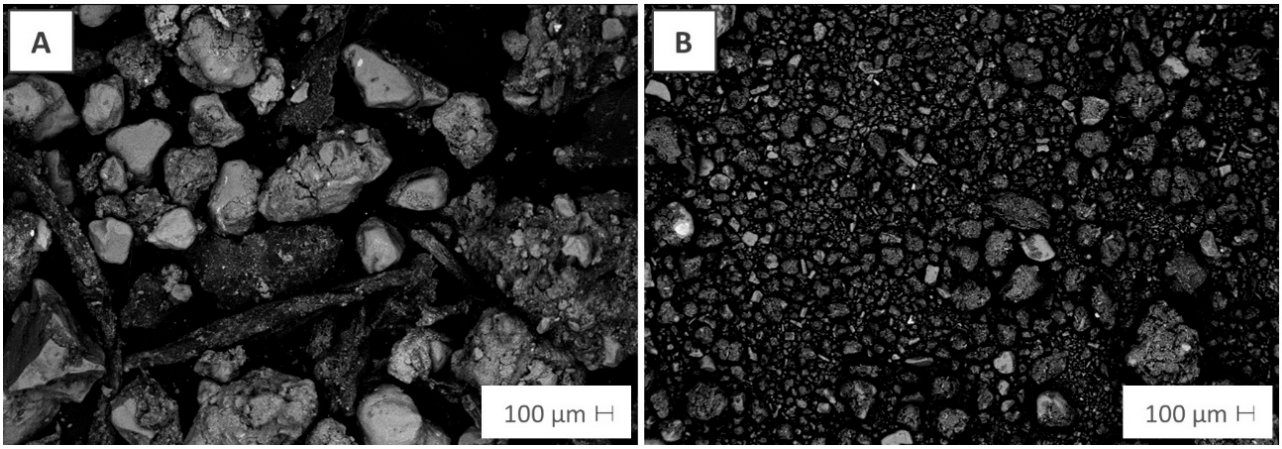

Figure 1. Photomicrographs of compost (**A**) and peat (**B**) by scanning electron microscopy (SEM).

The surface examination using EDS associated with SEM is illustrated in Figure 2. The results of the elementary analysis of EDS showed that C, O, Si, Al, and Fe were the main elements in the structure of both materials; however, the intensity was different, which confirms the data in Table 1 (elemental composition and XRF). For compost, Point 1 exhibited large concentrations of O and Si, possibly indicating the presence of quartz. Point 2, on the other hand, revealed an intense concentration of C combined with inorganic components (e.g., Al, Si, Fe, and Ca), probably indicating an aggregate of organic and inorganic matter (Figure 2A). For peat, Point 1 had a high C content, although inorganic elements (e.g., Si, Al, Ti, and Fe) were also present. In Point 2, the presence of C was lower due to the increase in the levels of inorganic constituents (mainly Ti and Fe). Thus, the samples illustrate an association between organic and inorganic plots typical of this material typology. In other words, peat is predominantly made up of inorganic portions coated with organic matter.

Regarding the surface functional group characterization, the FTIR spectra of the biosorbents compost and peat were obtained in the spectral range of 400 to 4000 cm^{-1}. The results showed that the compost and peat had different organic functional groups (Figure 3). Spectral bands close to 3440 and 3383 cm^{-1} for compost and peat, respectively, could indicate the presence of hydroxyl groups (–OH) based on the stretching vibrations present in alcohols, carboxylics and/or phenols [112,113]. Soobhany et al. [114] and Liu et al. [115] suggested that spectral bands in this range may also be indicative of N–H stretching vibrations associated with primary and secondary amines. In biosorbents, this characteristic peak may be associated with macromolecules, such as cellulose, lignin, and pectin, or absorbed water [26].

The subsequent appearance of two bands for peat (located at 2923 and 2846 cm^{-1}) and one band for compost (at 2923 cm^{-1}) might be attributed to the asymmetric and symmetrical stretching of the C–H group of long-chain aliphatic components.

The intense vibration peaks found at 1645 for compost and 1613 for peat could be from C–O stretching vibrations of the nonionic carboxyl (i.e., –COOH, $–COOCH_3$), which might be linked with carboxylic acids and/or ester groups of the lipids. Peaks at 1707 and 1639 cm^{-1} could also correspond to the formation of ketones, aldehydes, and carboxylic acid [114].

Aromatic substances accounted for the bands at approximately 1490 cm^{-1}. These structures may have been formed during composting [115] or in the decomposition of organic matter during peat formation. According to Chwastowski et al. [113], peaks in the bands between 1500 and 1650 cm^{-1} could represent aromatic C=C bonds associated with the presence of lignin.

The spectral bands at 1383 and 1390 cm^{-1} for compost and peat, respectively, possibly indicate the carboxylic groups (COO^-) of hemicellulose, pectin, and/or proteins [26]. C–O stretching of the polysaccharide structure or C–C stretching vibrations of aliphatic groups

were observed for compost and peat at bands of 1000 to 1100 cm^{-1} [115]. The peaks observed in wavenumbers in the range of 690 to 900 might be due to stretching vibrations of $–NH_2$ in proteins [26] or to deformation in the plane and outside the aromatic C–H plane [112].

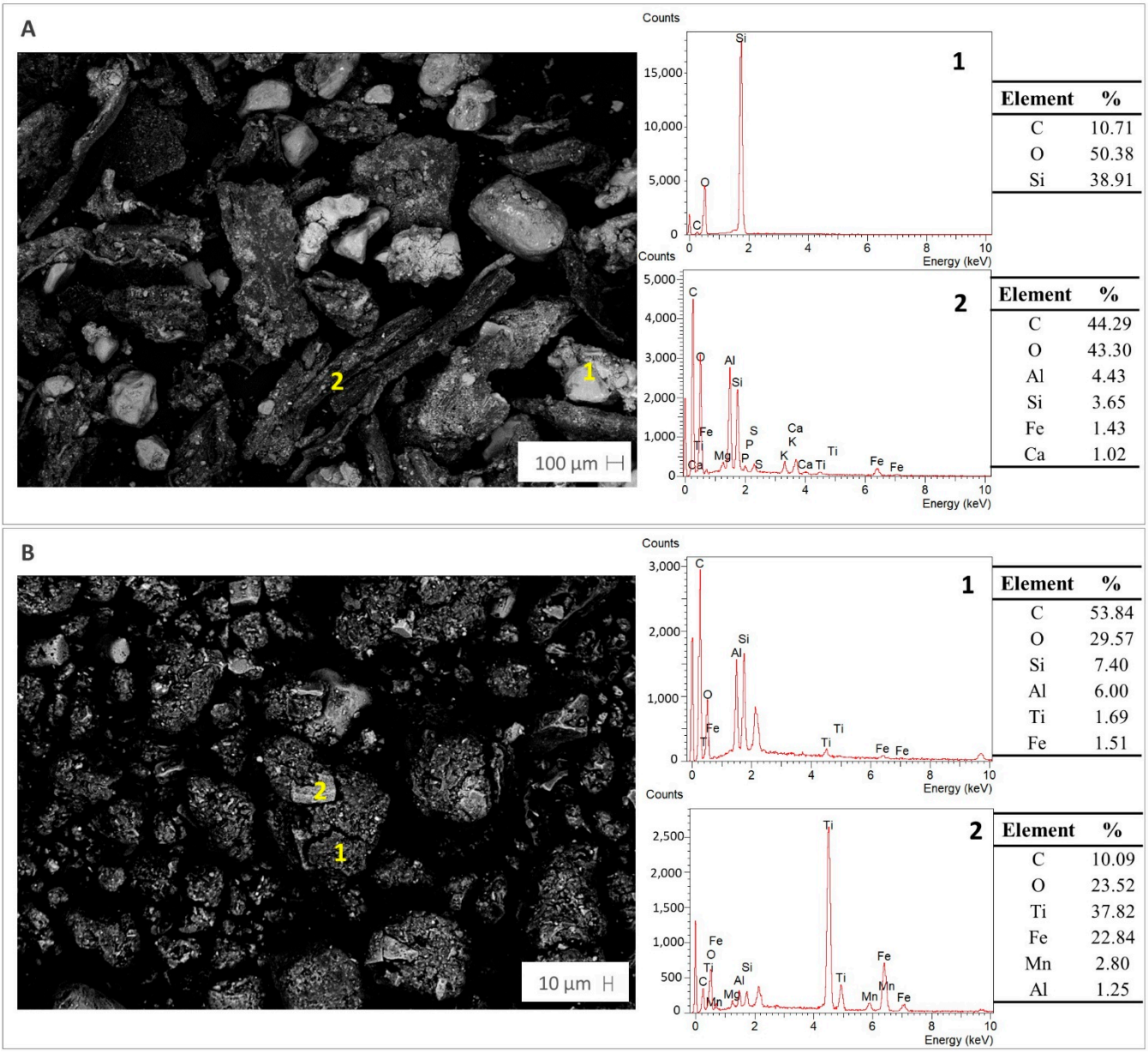

Figure 2. Photomicrographs of compost (**A**) and peat (**B**) by scanning electron microscopy (SEM) and X-ray energy dispersive spectroscopy (EDS) at two distinct points (1 and 2).

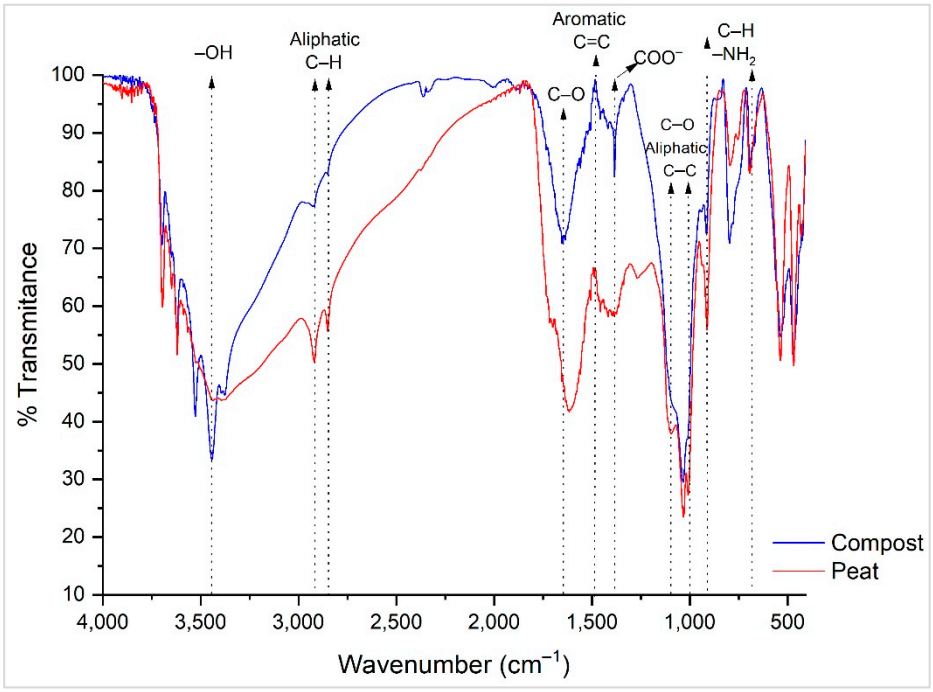

Figure 3. Infrared spectra of compost and peat.

Surface functional groups, mainly carbon-oxygen, are the most important structures influencing the surface behavior of sorbents and could be involved in Zn, Pb and/or Cd sorption.

Compost and peat have a wide pore size distribution and, consequently, a wide variation in specific surface area, confirming the SEM data. The pore volume and the surface area are positively correlated with the pore radius; that is, an increase in the radius implies an increase in the volume and/or the surface area. Compost had a slightly higher BET surface area than peat (5.689 vs. 3.451 m^2 g^{-1}, respectively; Table 2).

Table 2. SSA and pore distribution of compost and peat.

Parameter	Compost	Peat
SSA (m^2 g^{-1})		
(i) BET	5.689	3.451
(ii) BJH		
(a) Sorption cumulative	6.636	5.828
(b) Desorption cumulative	9.787	9.679
BJH V_p (cm^3 g^{-1})		
(i) BJH sorption	0.03412	0.02682
(ii) BJH desorption	0.03448	0.02783
R_p (Å)		
(i) BJH sorption	18.93	21.16
(ii) BJH desorption	94.24	18.73

SSA: specific surface area; V_p: total pore volume; R_p: average pore radius.

The BJH sorption pore distribution showed that peat has a greater SSA associated with a pore with a radius of up to 60 Å compared with compost, which had a greater SSA associated with a pore with a radius greater than 60 Å in relation to peat. However, peat has a larger average pore radius than compost (21.16 and 18.93 Å, respectively). Considering the IUPAC pore classification, the compost and peat do not have micropores (R_p < 10 Å) but rather have total pore areas composed of mesopores (10 Å < R_p < 250 Å) of 96.7 and 96.5%,

respectively, and macropores (R > 250 Å) of approximately 3.3% and 3.5%, respectively [116]. Therefore, both sorbents are predominantly mesoporous. Importantly, these results were consistent with and complemented those of the scanning electron micrographs of compost and peat, which were used to visualize the presence of pores in both materials.

3.2. Sorption Results

3.2.1. Equilibrium Studies

pH affects the overall performance of sorption mechanisms by directly interfering with the sorbent surface charges and ionization and speciation of the sorbate in solution. It has been reported that pH influences the uptake of PTE ions from aqueous solution; thus, it is important to determine the so-called optimum pH values for the sorption process, i.e., the value that maximizes contaminant sorption. However, in this research, the objective was to assess the behavior of the compost and peat under original conditions; therefore, pH variations were not assessed and the pH values were not adjusted at any time during the batch equilibrium test.

Considering peat, some studies have indicated that a pH range between 4.5 and 7.0 would be associated with the optimization of PTE sorption [35,117–119]. In the present study, the pH in the peat tests was in this interval, with results ranging from approximately 4.0 to 5.5, which may be considered a favorable characteristic, mainly for peat use under natural conditions. Under these pH conditions, approximately 90 to 99% of the hydrogen ions in COOH groups are dissociated, thus contributing positively to ion exchange reactions [101]. As the compost had a higher natural pH, this sorbent showed higher results for this parameter in the batch equilibrium test, with values from 5.0 to 6.5. In conditions of low pH, the high concentration of H^+ in aqueous solution competes with PTE ions for sorption sites (ion exchange); in conditions of high pH, the precipitation of metal oxides is the main mechanism of immobilization [34].

Based on Figure 4, the tests with Pb and Cd sorption on peat and compost, which precisely revealed the highest percentages of sorption, showed an increase in pH (comparing the initial pH with the respective pH at equilibrium). This increase can be explained by the release of hydroxyl ions (OH^-) by the sorbents [120] or by proton binding of the solution by the reactive materials [121]. It is also plausible to assume that this increase in pH may be due to the dissolution of components or ions present in the compost and peat. In contrast, in tests with Zn, mainly for the highest initial concentrations, a drop in pH was observed after contact of the peat and the compost with the contaminating aqueous solution. Ho et al. [122] and Bartczak et al. [119] associated this pH decrease with complexation and ion exchange through the deprotonation of sorbent functional groups. Hence, as more H^+ ions are released into the solution, more sites on the sorbent surface become free and the aqueous solution pH becomes lower. Another hypothesis presented by Gosset et al. [123] is that this drop is related to the acidic properties of the carboxylic and phenolic groups present in the peat humic substances. Given the difference in pH variation for the PTE studied (Zn, Cd and Pb), it is possible that different sorption mechanisms may act concurrently in the retention of each of these elements in the compost and peat.

Significantly, all sorption experiments occur under oxidizing conditions (see the Eh data in Figure 4). A comparison of the initial and equilibrium Eh values showed that the Eh value decreased, although the difference was not as significant in some samples (Figure 4). This could possibly be ascribed to the electron transfer controlled by aeration and biological reactions (the organic matter in both peat and compost may be an electron source).

The combined assessment of the pH and Eh data using characteristic diagrams of Zn, Pb and Cd indicated that these elements were predominantly in the cationic forms: Zn^{2+}, Pb^{2+} and Cd^{2+} in aqueous solutions during all sorption experiments (Figure 4).

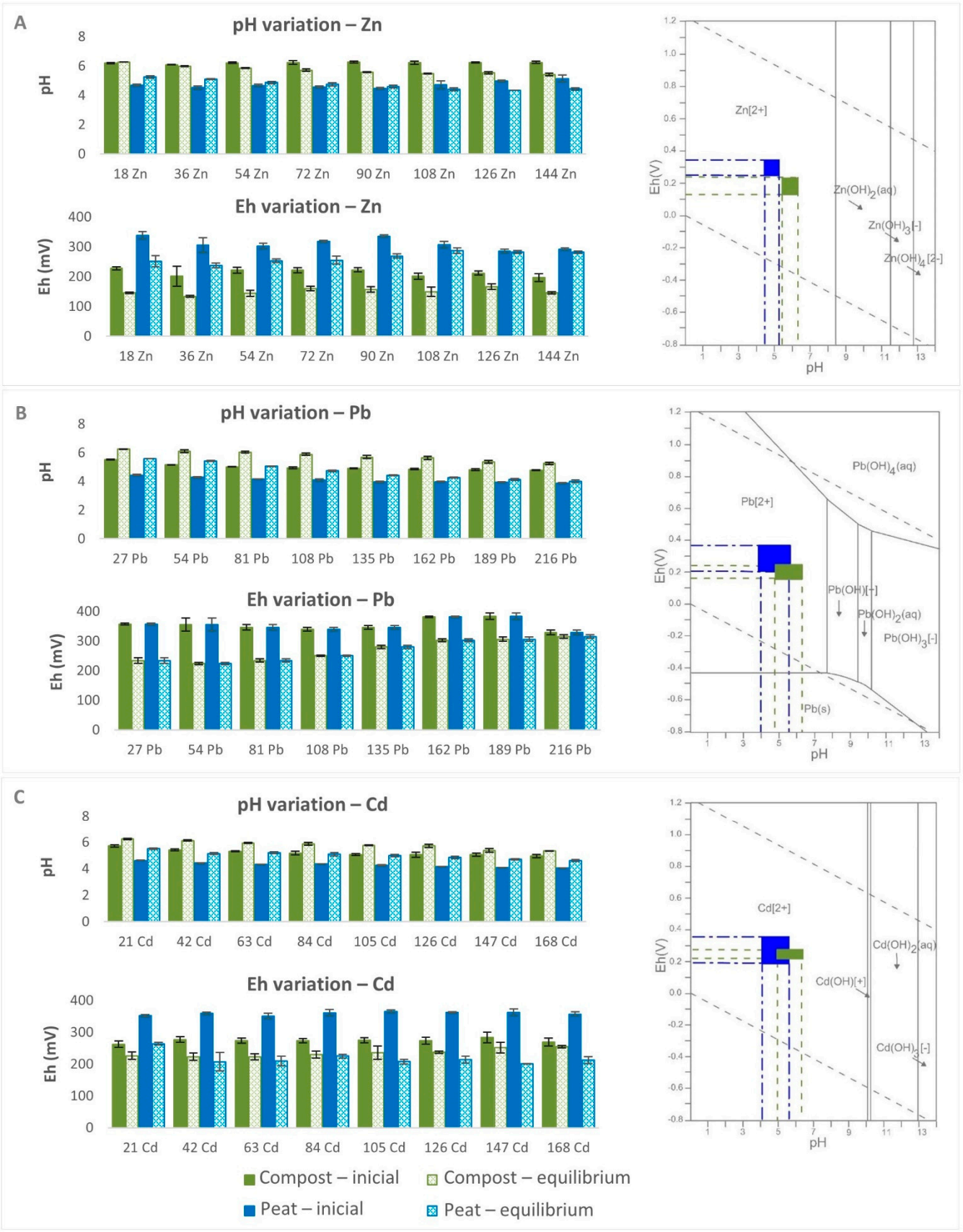

Figure 4. Initial and final pH and Eh values for compost and peat contaminated with Zn (**A**), Pb (**B**) and Cd (**C**). Each result is the mean ± standard deviation (vertical lines) for triplicate experiments (data entered in Brookins diagrams [124]).

The influence of different concentrations on the sorption of Zn, Pb and Cd by the compost and peat was tested, and the trends are illustrated in Figure 5. Comparing the sorbed concentration to the initial concentration, the highest percentage of removal was observed at the lowest concentrations, with removal values close to 100%. However, for the highest concentrations, the order of removal was Pb > Cd > Zn for compost and peat. Several mechanisms act on the sorption of PTE, but each does not attract different ions equally. Thus, an important factor in the evaluation of sorption is the affinity of each PTE for the sorbent [36].

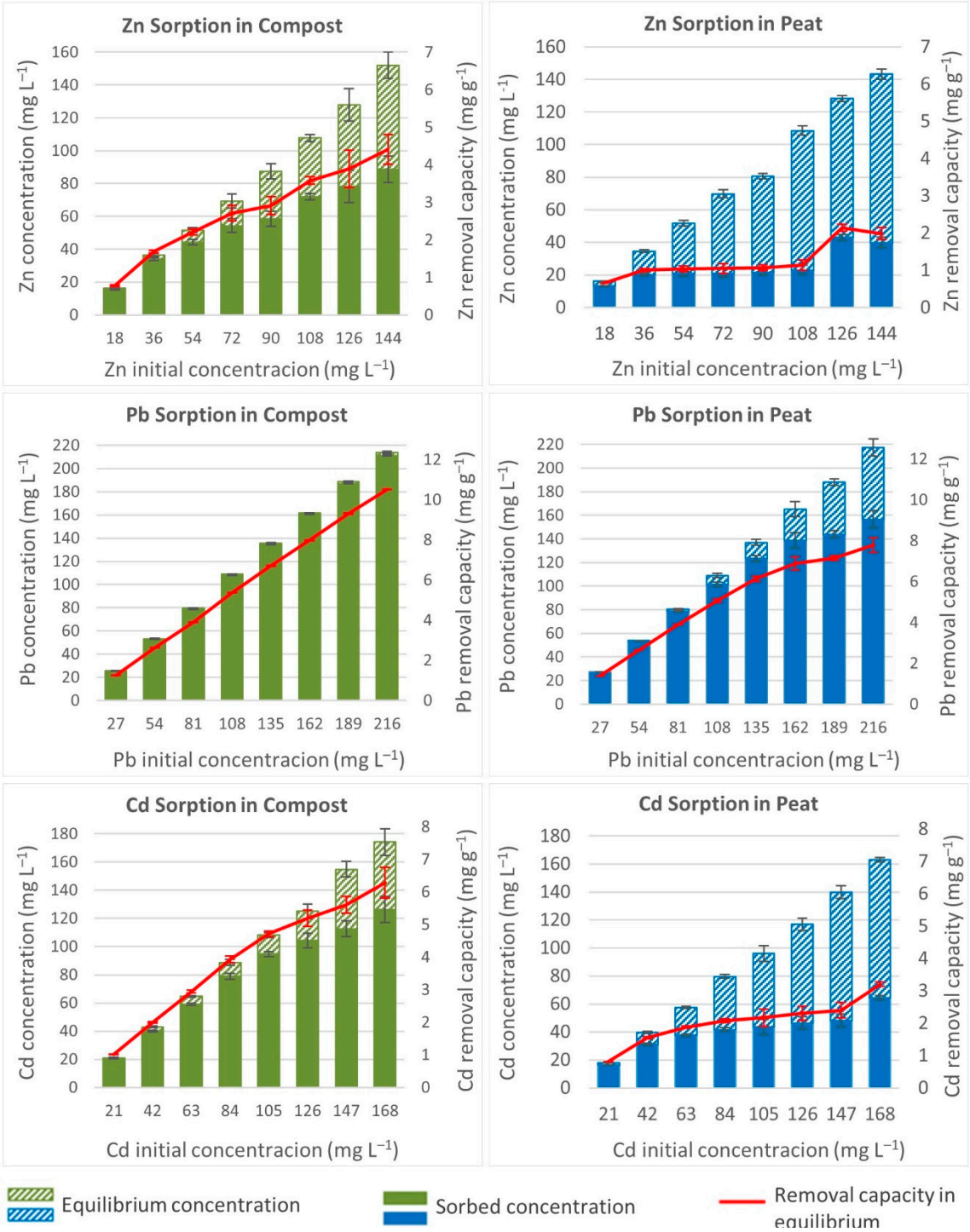

Figure 5. Batch test results showing the equilibrium and sorbed concentrations and removal capacity of compost and peat in contact with Zn, Pb and Cd. Each value is the mean ± standard deviation (vertical lines) for triplicate experiments.

The sorption of cations in solution is directly related to the attraction between negative surface charges and positive charges of ions [125]. Qin et al. [118] reported that the sorption affinity is associated with electronegativity and smoothness. In relation to electronegativity, the more electronegative the PTE ions are, the more strongly they will be attracted to the surface of the sorbent [126]. The order of affinity and the order of electronegativity (Pb: 2.33 > Cd: 1.69 > Zn: 1.65 [127]) were the same, thus confirming the assumptions of McKay and Porter [126]. The theory of hard and soft acids and bases (HSAB) states that so-called "class C cations" (including Pb) have the ability to form stronger complexes with fulvic and humic acids compared to "class B cations" (such as Zn and Cd) [37,128]. This could explain the great affinity of Pb with the compost and peat (Figure 5). In addition, the differences in the sorption behavior of Pb and Cd could be partially explained by the electronic configurations, with Pb presenting unpaired electrons that are more easily shared and empty spaces in its orbital, thus favoring the formation of complexes with sorbents [129]. Zn and Cd form complexes that are more unstable due to their low-spin configuration [37].

The removal capacity in the equilibrium of both materials was calculated as a function of the initial concentration of Zn, Pb and Cd, and the results are shown in Figure 5. It was noted that sorption increased with increasing initial concentration for all elements. The compost reached maximum values of 4.409, 10.511, and 6.287 mg g^{-1} in batch experiments with the highest initial concentrations of Zn, Pb, and Cd, respectively. However, the peat showed lower maximum removal capacities of 1.983, 7.778, and 3.202 mg g^{-1} for Zn, Pb, and Cd, respectively. A comparison of these sorption capacities with data for various sorbents indicated that the compost used in this study possessed a relatively high sorption capacity; thus, it presented a remarkable potential for the removal of Pb and Cd from aqueous solutions.

3.2.2. Kinetic Studies

The contact time is considered an important parameter that affects the sorption capacity of the sorbents and is determined by sorption kinetics. The contact time is a criterion widely used to identify the speed of binding and removal processes and to obtain the optimum time for the complete removal of the target ions.

For the compost and peat, the kinetic data (Table 3 and Figure 6) showed that the compost had a high removal capacity and achieved a faster equilibrium. For Pb removal, the compost attained equilibrium after 30 min, with a q determined experimentally (q_{exp}) of 9.392 mg g^{-1}; and for Cd and Zn removal, it attained equilibrium after 60 min (q_{exp} of 10.527 mg g^{-1}) and 120 min (q_{exp} of 11.278 mg g^{-1}), respectively. The peat required approximately 210 min for equilibrium of the three potentially toxic elements, achieving q_{exp} values of 8.177, 4.466, and 3.061 mg g^{-1} for Pb, Cd, and Zn, respectively. The same pattern between a composted material and a peat for the kinetic data was revealed by Raimondi et al. [130], in which study, the composted agro-based waste material (from sugarcane crops) achieved faster equilibrium for Pb and Zn removal (requiring 30 and 60 min, respectively), while the peat needed nearly 180 and 90 min for the potentially toxic elements, respectively.

Shah et al. [131] also reported the rapidness of a composted material (prepared from biodegradable fractions of MSW) for the removal of Pb from contaminated water, with a fast uptake within the first 30 min. According to these authors, the highly porous structure of the compost provides complete access and a large surface for Pb sorption at the binding sites.

The velocity at which the target ions were removed also serves as the basis for understanding the process mechanism. Therefore, the experimental data of the sorption kinetics were fitted to the PSO, PFO, Elovich, M&W, and W&M models to provide additional insights into the potential rate-controlling steps and mechanisms of the sorption process. The results of kinetics data modeling are summarized in Table 3, and they revealed that

both materials had different behaviors and even differences regarding the potentially toxic elements analyzed.

Table 3. Kinetic parameters for the sorption of Pb, Cd, and Zn on compost and peat at 220 mg L^{-1}.

Model	Parameters	Compost			Peat		
		Zn	Pb	Cd	Zn	Pb	Cd
	q_{exp} (mg g^{-1})	11.278	9.392	10.527	3.061	8.177	4.466
	Equilibrium time (min)	120	30	60	210	210	210
PFO	$q_{e(1)}$ (mg g^{-1})	10.933	9.354	10.425	2.922	8.132	4.479
	k_1 (min^{-1})	0.057	3.123	0.108	0.061	0.022	0.012
	R^2	0.970	0.998	0.981	0.853	0.931	0.923
	SSE	6.177	0.194	3.409	2.468	8.820	2.918
PSO	$q_{e(2)}$ (mg g^{-1})	11.660	9.392	10.655	3.135	9.101	4.941
	k_2 (mg g^{-1} min^{-1})	0.008	0.383	0.029	0.029	0.003	0.004
	R^2	0.991	0.999	0.987	0.877	0.958	0.935
	SSE	1.793	0.087	2.223	2.037	4.997	2.203
Elovich	α (mg g^{-1} min^{-1})	21.669	1600.052	212.278	400.801	2.239	0.391
	β (mg g^{-1})	0.751	1.366	1.020	4.448	0.789	1.248
	R^2	0.961	0.921	0.945	0.961	0.949	0.918
	SSE	7.411	9.064	8.315	0.392	5.567	2.564
M&W	$k_{M\&W}$ S (cm min^{-1} cm^{-1})	0.038	3.041	0.070	0.001	0.012	0.001
	R^2	0.938	0.994	0.926	0.544	0.913	0.655
	SSE	16.907	0.698	18.888	46.698	14.921	48.066
W&M	$k_{W\&M}$ (mg g^{-1} $min^{-0.5}$)	0.554	0.447	0.529	0.151	0.396	0.198
	R^2	0.620	0.556	0.578	0.632	0.704	0.726
	SSE	266.014	282.744	307.417	19.379	89.302	19.622

For the compost, the R^2 values of Pb, Cd, and Zn for the PSO, PFO, and Elovich models remained above 0.90 (SSE below 9.100), thus establishing good adjustments for each model under consideration. The PSO model showed high R^2 (above 0.987) and low SSE (below 2.223) over PFO (R^2 above 0.970, and SSE below 6.177). In addition, the sorption capacities for PSO ($q_{e(2)}$) were consistent with the experimental data (q_{exp}). The consensus for the three parameters may assume that the rate-limiting step is chemical or physicochemical adsorption, which involves the transfer, exchange, and cooccurrence of electrons [132]. In biosorbents (such as compost), chemisorption may occur between the functional groups of organic matter (mainly OH^-) and cations, with PSO widely applicable to kinetic data of biosorption systems [133]. Through the Elovich equation, it is possible to infer that the compost surface is heterogeneous (energetically).

Regarding the results of the diffusion models, the M&W model presented a good fit for the compost data ($R^2 > 0.920$), indicating that the external mass transfer process plays an important role in the sorption process. The differences between the bulk solution and sorbent surface concentrations were considered the driving force of external diffusion (through the liquid film); therefore, at 220 mg L^{-1}, the number of external binding sites of the compost was considered sufficient to sorb Pb, Cd, and Zn, and quick equilibrium was achieved. Regarding the W&M model, the R^2 and SSE values for the compost (Table 3) did not confirm that the sorption rate-limiting step was the intraparticle diffusion process for the analyzed data. However, the multilinearity of the plots (Figure 6) indicated that intraparticle diffusion also played a role in the uptake of the PTE (especially Zn and Cd) by this material. In the first stage, the steepest portion of the curve relates to almost instantaneous external surface sorption. The second stage is gradual sorption, when intraparticle diffusion occurs. The third stage assumes that sorption equilibrium has been achieved and that the smallest PTE in solution causes a decrease in intraparticle diffusion [134].

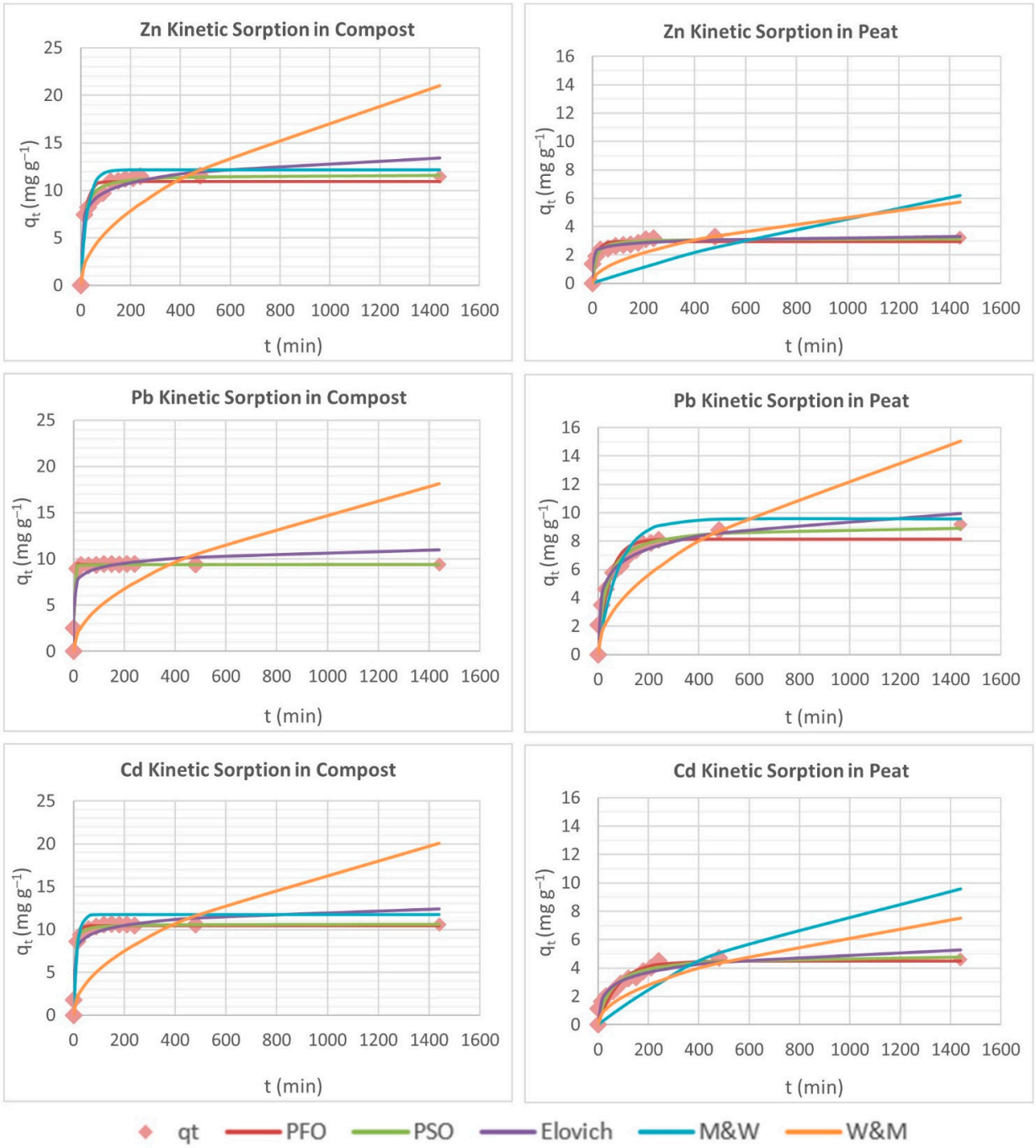

Figure 6. Kinetic experimental data of sorption of Pb, Cd, and Zn on peat and compost, and their adjustments to PFO, PSO, Elovich, M&W, and W&M models.

Peat, on the other hand, showed different behavior depending on the potentially toxic element. Pb and Cd exhibit a better fit with the PSO model (R^2 of 0.958 and 0.935 and SSE of 4.997 and 2.203, respectively). For both PTEs, the R^2 values for the PFO and Elovich models also remained above 0.90, assuming the same conditions as for compost (chemisorption and peat energetically heterogeneous surface). Regarding the diffusion models, the adjustment of the M&W model to the Pb data was highlighted, thus indicating a relevant contribution of the external mass transfer process. In this situation, due to the high sorption affinity of the peat for Pb, the external binding sites were efficient in sorbing the available Pb. However, as also observed for the compost, the multilinearity of the plots (Figure 6) indicated the occurrence of both mass transfer (external and intraparticle

diffusion). Physically, when the external binding sites were occupied by Zn, Pb, and Cd, the additional cations migrated to pore spaces within the peat. See Figure 7.

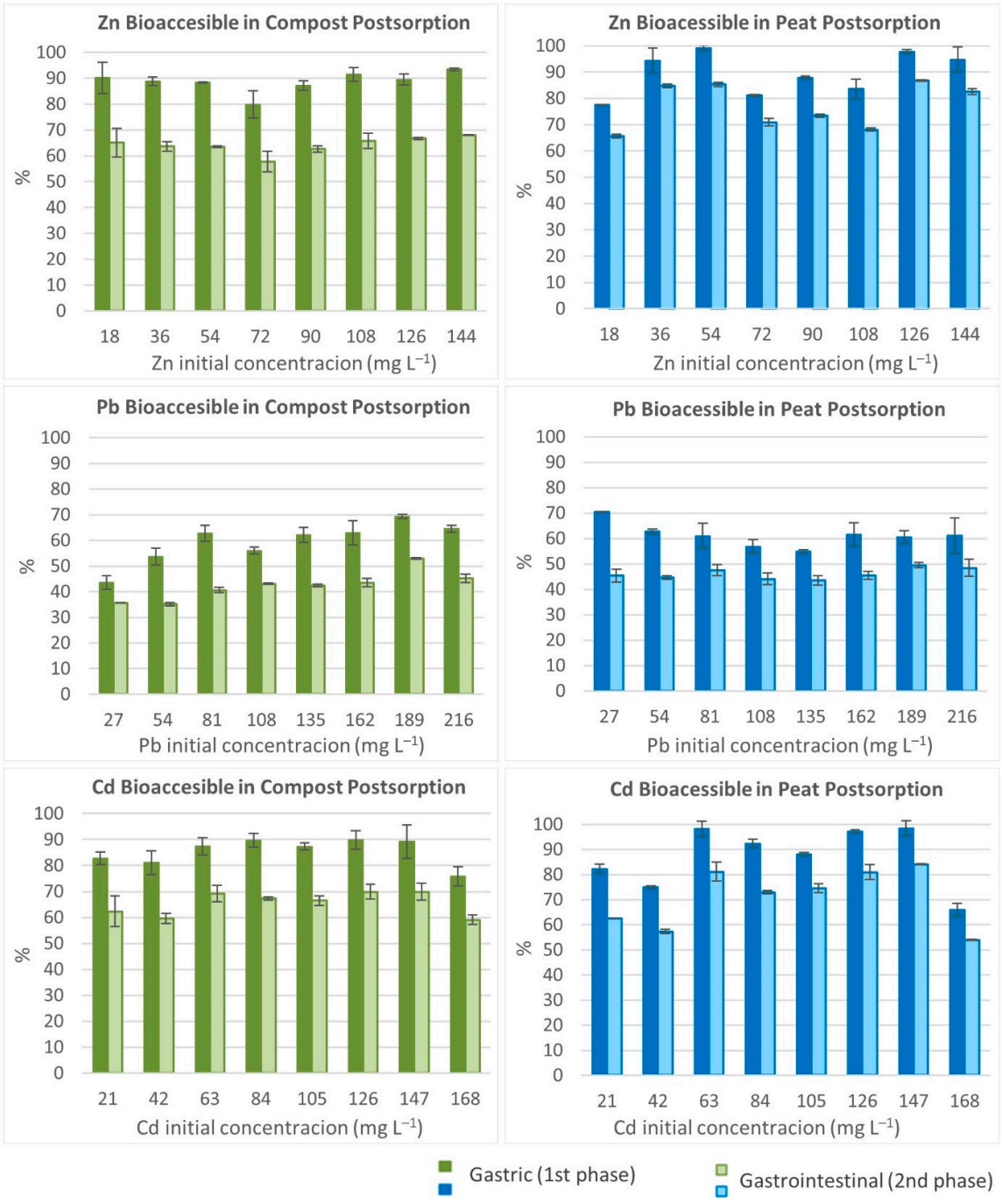

Figure 7. Zn, Pb and Cd bioaccessible concentrations (gastric and gastrointestinal phases) in compost and peat postsorption. Each value is the mean ± standard deviation (vertical lines) for duplicate experiments.

3.3. Human Bioaccessibility

Regarding the risk assessment for human health, oral intake is the main exposure route to contaminants [63]. Thus, there is a need to use a practical methodology to measure the contaminant fraction that can enter the human blood system, causing toxic effects [64]. In this context, the impacts of peat and compost ingestion after sorption of Zn, Pb and Cd were simulated using the in vitro bioaccessibility test (Figure 7). In a real situation, these saturated reactive materials used in the treatment of contaminated effluents or as

organic amendments in the remediation of soil contaminated with PTE could be exposed to weathering or directly and indirectly ingested by local adults and children (associated with food and/or water).

The experimental results for human bioaccessibility showed higher concentrations in the first stage, simulating the acidic conditions in the stomach (pH~1.5), than in the second phase, simulating uptake by the human intestine (increase in pH close to neutral values). The bioaccessible fractions in the first stage were greater than 80%, 50% and 70% for Zn, Pb and Cd, respectively, thus indicating potential risks to human health. Notably, among the PTE targets of this study, Pb had the highest sorption percentages (Figure 5) and the lowest bioaccessibility (Figure 7).

These results are consistent with previous studies that have already highlighted the importance of bioaccessibility tests in the evaluation of potential sorbents. Lima et al. [135] obtained higher bioaccessible Cd fractions for the gastric phase of postsorption Brazilian peats that were previously activated with HCl. Raimondi et al. [25] reported the bioaccessibility of 92% of the Cd sorbed on composted sugarcane pressmud in a batch test with a concentration of 500 mg L^{-1}. Raimondi et al. [130] showed higher bioaccessible percentages of Zn and Pb for organic materials, peat and pressmud (greater than 80%) compared to zeolites (less than 30%).

4. Conclusions

This study indicated that compost and peat have good potential as low-cost, ecofriendly sorbents for the immobilization of Zn, Pb and Cd. The compost reached removal of 99.7%, 72.5% and 58.3% in batch experiments with the highest initial concentrations of Pb, Cd and Zn, respectively. However, the peat showed lower removal of 71.9%, 39.5% and 27.8% for Pb, Cd and Zn, respectively. Kinetic sorption is very fast, principally for compost, and equilibrium conditions are reached in minutes (e.g., 30 min for Pb sorption into compost). The PSO model provided the best fit for the equilibrium from compost, indicating chemisorption as the rate-limiting step. However, the PFO and Elovich models were also well fitted, thus demonstrating that the peat and compost surfaces were energetically heterogeneous. In addition, the external (M&W) and intraparticle (W&M) diffusion models used here also showed a good fit, mainly for the sorption of Zn, Pb and Cd in compost and Pb in peat, thus indicating the participation of diffusion in the dominant sorption mechanisms. The human bioaccessibility data showed higher concentrations in the first phase (pH~1.5) than in the second phase (pH~7.0). The bioaccessible fractions in the first stage were lower for Pb (between 40% and 70%) than Zn and Cd (between 75% and 95%), thus indicating potential risks to human health. The overall findings indicated that the compost exhibited the best results mainly for Pb sorption. This material stands out because it is derived from OFMSW, which is cheap and abundant, and its use in the recovery of contaminated areas represents a solution for OFMSW management, thus providing added value based on a circular economy.

Author Contributions: Conceptualization: J.Z.L., V.G.S.R.; Methodology: J.Z.L., R.M.L.; Investigation: J.Z.L., R.M.L., I.M.R., V.G.S.R.; Writing—original draft preparation: J.Z.L., I.M.R.; Writing—review and editing: J.Z.L., I.M.R., O.J.P., V.G.S.R.; Resources: O.J.P., V.G.S.R.; Supervision, V.G.S.R. All authors have read and agreed to the published version of the manuscript.

Funding: The authors would like to acknowledge the São Paulo Research Foundation (FAPESP) for providing Master and PhD scholarships (process numbers 2015/02529-4 and 2017/16961-0) and financial support (2014/07180-7) and the National Council for Scientific and Technological Development (CNPq) for the Research Productivity Fellow ship (310989/2020-5 and 302987/2017-7).

Institutional Review Board Statement: Not applicable.

Informed Consent Statement: Not applicable.

Data Availability Statement: Not applicable.

Conflicts of Interest: The authors declare no conflict of interest.

References

1. Mohamed, A.M.O.; Paleologos, E.K.; Rodrigues, V.G.S.; Singh, D.N. *Fundamentals of Geoenvironmental Engineering: Understanding Soil, Water, and Pollutant Interaction and Transport*; Elsevier: Amsterdam, The Netherlands, 2017; ISBN 9780128051450.
2. Förstner, U.; Wittmann, G.T.W. *Metal Pollution in the Aquatic Environment*; Springer: Berlin/Heidelberg, Germany; New York, NY, USA; Tokyo, Japan, 1983.
3. Kabata-Pendias, A. *Trace Elements in Soils and Plants*, 4th ed.; CRC Press LLC: Boca Raton, MA, USA; London, UK; New York, NY, USA, 2011.
4. Boscov, M.E.G. *Geotecnia Ambiental*; Oficina de Textos: São Paulo, Brazil, 2008.
5. Bosso, S.T.; Enzweiler, J. Bioaccessible lead in soils, slag, and mine wastes from an abandoned mining district in Brazil. *Environ. Geochem. Health* **2007**, *30*, 219–229. [CrossRef]
6. Ettler, V.; Tomášová, Z.; Komárek, M.; Mihaljevič, M.; Šebek, O.; Michálková, Z. The pH-dependent long-term stability of an amorphous manganese oxide in smelter-polluted soils: Implication for chemical stabilization of metals and metalloids. *J. Hazard. Mater.* **2015**, *286*, 386–394. [CrossRef] [PubMed]
7. Ettler, V.; Cihlová, M.; Jarošíková, A.; Mihaljevič, M.; Drahota, P.; Kříbek, B.; Vaněk, A.; Penížek, V.; Sracek, O.; Klementová, M.; et al. Oral bioaccessibility of metal(loid)s in dust materials from mining areas of northern Namibia. *Environ. Int.* **2019**, *124*, 205–215. [CrossRef]
8. Kasemodel, M.C.; Lima, J.Z.; Sakamoto, I.K.; Varesche, M.B.A.; Trofino, J.C.; Rodrigues, V.G.S. Soil contamination assessment for Pb, Zn and Cd in a slag disposal area using the integration of geochemical and microbiological data. *Environ. Monit. Assess.* **2016**, *188*, 1–24. [CrossRef]
9. Kasemodel, M.C.; Papa, T.B.R.; Sígolo, J.B.; Rodrigues, V.G.S. Assessment of the mobility, bioaccessibility, and ecological risk of Pb and Zn on a dirt road located in a former mining area-Ribeira Valley-Brazil. *Environ. Monit. Assess.* **2019**, *191*, 101. [CrossRef]
10. Kasemodel, M.C.; Sakamoto, I.K.; Varesche, M.B.A.; Rodrigues, V.G.S. Potentially toxic metal contamination and microbial community analysis in an abandoned Pb and Zn mining waste deposit. *Sci. Total Environ.* **2019**, *675*, 367–379. [CrossRef] [PubMed]
11. Helser, J.; Cappuyns, V. Trace elements leaching from Pb-Zn mine waste (Plombières, Belgium) and environmental implications. *J. Geochem. Explor.* **2021**, *220*, 106659. [CrossRef]
12. Orgiazzi, A.; Bardgett, R.D.; Barrios, E.; Behan-Pelletier, V.; Briones, M.J.I.; Chotte, J.-L.; De Deyn, G.B.; Eggleton, P.; Fierer, N.; Fraser, T.; et al. *Global Soil Biodiversity Atlas*; European Commission, Publications Office of the European Union: Luxembourg, 2016.
13. World Health Organization (WHO). *Environmental Health Criteria 221 ZINC*; WHO: Geneva, Switzerland, 2001.
14. Agency for Toxic Substances and Diseases Registry (ATSDR). *Toxicological Profile for Zinc*; ATSDR: Atlanta, GA, USA, 2005.
15. Agency for Toxic Substances and Diseases Registry (ATSDR). *Toxicological Profile for Lead*; ATSDR: Atlanta, GA, USA, 2020.
16. Boskabady, M.; Marefati, N.; Farkhondeh, T.; Shakeri, F.; Farshbaf, A.; Boskabady, M.H. The effect of environmental lead exposure on human health and the contribution of inflammatory mechanisms, a review. *Environ. Int.* **2018**, *120*, 404–420. [CrossRef]
17. Agency for Toxic Substances and Diseases Registry (ATSDR). *Toxicological Profile for Cadmium*; ATSDR: Atlanta, GA, USA, 2012.
18. Tian, J.; Li, Z.; Wang, L.; Qiu, D.; Zhang, X.; Xin, X.; Cai, Z.; Lei, B. Metabolic signatures for safety assessment of low-level cadmium exposure on human osteoblast-like cells. *Ecotoxicol. Environ. Saf.* **2021**, *207*, 111257. [CrossRef]
19. U.S. Environmental Protection Agency (US EPA). *Abandoned Mine Site Characterization and Cleanup Handbook*; US EPA: Washington, DC, USA, 2000.
20. Božić, D.; Stanković, V.; Gorgievski, M.; Bogdanović, G.; Kovačević, R. Adsorption of heavy metal ions by sawdust of deciduous trees. *J. Hazard. Mater.* **2009**, *171*, 684–692. [CrossRef]
21. Alhogbi, B.G. Potential of coffee husk biomass waste for the adsorption of Pb(II) ion from aqueous solutions. *Sustain. Chem. Pharm.* **2017**, *6*, 21–25. [CrossRef]
22. Adewuyi, A.; Pereira, F.V. Underutilized Luffa cylindrica sponge: A local bio-adsorbent for the removal of Pb(II) pollutant from water system. *Beni Suef Univ. J. Basic Appl. Sci.* **2017**, *6*, 118–126. [CrossRef]
23. Çelebi, H.; Gök, G.; Gök, O. Adsorption capability of brewed tea waste in waters containing toxic lead(II), cadmium (II), nickel (II), and zinc(II) heavy metal ions. *Sci. Rep.* **2020**, *10*, 1–12. [CrossRef]
24. Milani, P.A.; Debs, K.B.; Labuto, G.; Carrilho, E.N.V.M. Agricultural solid waste for sorption of metal ions: Part I—characterization and use of lettuce roots and sugarcane bagasse for Cu(II), Fe(II), Zn(II), and Mn(II) sorption from aqueous medium. *Environ. Sci. Pollut. Res.* **2018**, *25*, 35895–35905. [CrossRef]
25. Raimondi, I.M.; Rodrigues, V.G.S.; Lima, J.Z.; Marques, J.P.; Vaz, L.A.A. The Potential Use of Pressmud as Reactive Material for Cd2+ Removal: Adsorption Equilibrium, Kinetics, Desorption, and Bioaccessibility. *Water Air Soil Pollut.* **2020**, *231*, 365. [CrossRef]
26. Shakoor, M.B.; Niazi, N.K.; Bibi, I.; Shahid, M.; Saqib, Z.A.; Nawaz, M.F.; Shaheen, S.M.; Wang, H.; Tsang, D.C.W.; Bundschuh, J.; et al. Exploring the arsenic removal potential of various biosorbents from water. *Environ. Int.* **2019**, *123*, 567–579. [CrossRef]
27. Nie, C.; Yang, X.; Niazi, N.K.; Xu, X.; Wen, Y.; Rinklebe, J.; Ok, Y.S.; Xu, S.; Wang, H. Impact of sugarcane bagasse-derived biochar on heavy metal availability and microbial activity: A field study. *Chemosphere* **2018**, *200*, 274–282. [CrossRef] [PubMed]
28. He, L.; Zhong, H.; Liu, G.; Dai, Z.; Brookes, P.C.; Xu, J. Remediation of heavy metal contaminated soils by biochar: Mechanisms, potential risks and applications in China. *Environ. Pollut.* **2019**, *252*, 846–855. [CrossRef] [PubMed]

29. Li, Y.; Xing, B.; Ding, Y.; Han, X.; Wang, S. A critical review of the production and advanced utilization of biochar via selective pyrolysis of lignocellulosic biomass. *Bioresour. Technol.* **2020**, *312*, 123614. [CrossRef]
30. Lima, J.Z.; Ferreira da Silva, E.; Patinha, C.; Durães, N.; Vieira, E.M.; Silvestre Rodrigues, V.G. Sorption of arsenic by composts and biochars derived from the organic fraction of municipal solid wastes: Kinetic, isotherm and oral bioaccessibility study. *Environ. Res.* **2021**, *204*, 111988. [CrossRef]
31. Khoshand, A.; Fall, M. Geotechnical characterization of peat-based landfill cover materials. *J. Rock Mech. Geotech. Eng.* **2016**, *8*, 596–604. [CrossRef]
32. Marques, J.P.; Rodrigues, V.G.S.; Raimondi, I.M.; Lima, J.Z. Increase in Pb and Cd Adsorption by the Application of Peat in a Tropical Soil. *Water Air Soil Pollut.* **2020**, *231*, 365. [CrossRef]
33. Raimondi, I.M.; Rodrigues, V.G.; Lima, J.Z.; Marques, J.P.; Vaz, L.A.A.; Vieira, E.M. Assessment of the use of tropical peats as local alternative materials for the adsorption of Pb, Zn and Cd: An equilibrium study. *Earth Sci. Res. J.* **2021**, *25*, 29–40. [CrossRef]
34. Couillard, D. The use of peat in wastewater treatment. *Water Res.* **1994**, *28*, 1261–1274. [CrossRef]
35. Petroni, S.L.G. Adsorption Studies of Zinc and Cadmium on Peat. Potential Use of a Natural Biosorbent in Wastewater Treatment. Master's Thesis, Nuclear and Energy Research Institute (IPEN), Associated to the University of São Paulo (USP), São Paulo, Brazil, 1999.
36. Brown, P.A.; Gill, S.A.; Allen, S.J. Metal removal from wastewater using peat. *Water Res.* **2000**, *34*, 3907–3916. [CrossRef]
37. Kalmykova, Y.; Strömvall, A.M.; Steenari, B.M. Adsorption of Cd, Cu, Ni, Pb and Zn on Sphagnum peat from solutions with low metal concentrations. *J. Hazard. Mater.* **2008**, *152*, 885–891. [CrossRef]
38. Abat, M.; McLaughlin, M.J.; Kirby, J.K.; Stacey, S.P. Adsorption and desorption of copper and zinc in tropical peat soils of Sarawak, Malaysia. *Geoderma* **2012**, *175–176*, 58–63. [CrossRef]
39. Lee, S.J.; Lee, M.E.; Chung, J.W.; Park, J.H.; Huh, K.Y.; Jun, G.I. Immobilization of lead from Pb-contaminated soil amended with peat moss. *J. Chem.* **2013**, *2013*, 509520. [CrossRef]
40. Egene, C.E.; Van Poucke, R.; Ok, Y.S.; Meers, E.; Tack, F.M.G. Impact of organic amendments (biochar, compost and peat) on Cd and Zn mobility and solubility in contaminated soil of the Campine region after three years. *Sci. Total Environ.* **2018**, *626*, 195–202. [CrossRef]
41. Tang, C.; Chen, Y.; Zhang, Q.; Li, J.; Zhang, F.; Liu, Z. Effects of peat on plant growth and lead and zinc phytostabilization from lead-zinc mine tailing in southern China: Screening plant species resisting and accumulating metals. *Ecotoxicol. Environ. Saf.* **2019**, *176*, 42–49. [CrossRef]
42. Crescêncio Júnior, F. *A Study in Lab of Peats as a Reactive Barrier for Remediation of Aquifers*; Federal University of Rio de Janeiro (UFRJ): Rio de Janeiro, Brazil, 2008.
43. Koivula, M.P.; Kujala, K.; Rönkkömäki, H.; Mäkelä, M. Sorption of Pb(II), Cr(III), Cu(II), As(III) to peat, and utilization of the sorption properties in industrial waste landfill hydraulic barrier layers. *J. Hazard. Mater.* **2009**, *164*, 345–352. [CrossRef] [PubMed]
44. Gonzalez, A.G.; Pokrovsky, O.S.; Beike, A.K.; Reski, R.; Di Palma, A.; Adamo, P.; Giordano, S.; Angel Fernandez, J. Metal and proton adsorption capacities of natural and cloned Sphagnum mosses. *J. Colloid Interface Sci.* **2016**, *461*, 326–334. [CrossRef] [PubMed]
45. Wu, H.; Wen, Q.; Hu, L.; Gong, M.; Tang, Z. Feasibility study on the application of coal gangue as landfill liner material. *Waste Manag.* **2017**, *63*, 161–171. [CrossRef]
46. Vaverková, M.D.; Adamcová, D.; Winkler, J.; Koda, E.; Petrželová, L.; Maxianová, A. Alternative method of composting on a reclaimed municipal waste landfill in accordance with the circular economy: Benefits and risks. *Sci. Total Environ.* **2020**, *723*, 137971. [CrossRef]
47. Hoornweg, D.; Bhada-Tata, P. *What a Waste: A Global Review of Solid Waste Management*; World Bank: Washington, DC, USA, 2012.
48. Jara-Samaniego, J.; Pérez-Murcia, M.D.; Bustamante, M.A.; Paredes, C.; Pérez-Espinosa, A.; Gavilanes-Terán, I.; López, M.; Marhuenda-Egea, F.C.; Brito, H.; Moral, R. Development of organic fertilizers from food market waste and urban gardening by composting in Ecuador. *PLoS ONE* **2017**, *12*, e0181621. [CrossRef]
49. Kocasoy, G.; Güvener, Z. Efficiency of compost in the removal of heavy metals from the industrial wastewater. *EnGeo* **2009**, *57*, 291–296. [CrossRef]
50. Farrell, M.; Jones, D.L. Use of composts in the remediation of heavy metal contaminated soil. *J. Hazard. Mater.* **2010**, *175*, 575–582. [CrossRef]
51. Farrell, M.; Jones, D.L. Food waste composting: Its use as a peat replacement. *Waste Manag.* **2010**, *30*, 1495–1501. [CrossRef]
52. Farrell, M.; Perkins, W.T.; Hobbs, P.J.; Griffith, G.W.; Jones, D.L. Migration of heavy metals in soil as influenced by compost amendments. *Environ. Pollut.* **2010**, *158*, 55–64. [CrossRef]
53. Paradelo, R.; Barral, M.T. Evaluation of the potential capacity as biosorbents of two MSW composts with different Cu, Pb and Zn concentrations. *Bioresour. Technol.* **2012**, *104*, 810–813. [CrossRef] [PubMed]
54. Lima, J.Z.; Raimondi, I.M.; Schalch, V.; Rodrigues, V.G.S. Assessment of the use of organic composts derived from municipal solid waste for the adsorption of Pb, Zn and Cd. *J. Environ. Manag.* **2018**, *226*, 386–399. [CrossRef] [PubMed]
55. Abou Jaoude, L.; Garau, G.; Nassif, N.; Darwish, T.; Castaldi, P. Metal(loid)s immobilization in soils of Lebanon using municipal solid waste compost: Microbial and biochemical impact. *Appl. Soil Ecol.* **2019**, *143*, 134–143. [CrossRef]

56. Tang, J.; Zhang, L.; Zhang, J.; Ren, L.; Zhou, Y.; Zheng, Y.; Luo, L.; Yang, Y.; Huang, H.; Chen, A. Physicochemical features, metal availability and enzyme activity in heavy metal-polluted soil remediated by biochar and compost. *Sci. Total Environ.* **2020**, *701*, 134751. [CrossRef] [PubMed]
57. Haynes, R.J.; Naidu, R. Influence of lime, fertilizer and manure applications on soil organic matter content and soil physical conditions: A review. *Nutr. Cycl. Agroecosyst.* **1998**, *51*, 123–137. [CrossRef]
58. Epstein, E. *The Science of Composting*; CRC Press LLC: Boca Raton, FL, USA, 1997.
59. Hooda, P.S. Trace Elements in Soils. *Trace Elem. Soils* **2010**. [CrossRef]
60. Interstate Technology & Regulatory Council (ITRC). *Permeable Reactive Barriers: Lessons Learned/New Directions Technical/Regulatory Guidelines*; ITRC: Washington, DC, USA, 2005.
61. Bolan, N.; Kunhikrishnan, A.; Thangarajan, R.; Kumpiene, J.; Park, J.; Makino, T.; Kirkham, M.B.; Scheckel, K. Remediation of heavy metal(loid)s contaminated soils—To mobilize or to immobilize? *J. Hazard. Mater.* **2014**, *266*, 141–166. [CrossRef] [PubMed]
62. Naidu, R.; Semple, K.T.; Megharaj, M.; Juhasz, A.L.; Bolan, N.S.; Gupta, S.K.; Clothier, B.E.; Schulin, R. Chapter 3 Bioavailability: Definition, assessment and implications for risk assessment. *Dev. Soil Sci.* **2008**, *32*, 39–51. [CrossRef]
63. Paustenbach, D.J. The practice of exposure assessment: A state-of-the-art review. *J. Toxicol. Environ. Health Part B Crit. Rev.* **2000**, *3*, 179–291. [CrossRef]
64. Wragg, J.; Cave, M.R. *In-Vitro Methods for the Measurement of the Oral Bioaccessibility of Selected Metals and Metalloids in Soils: A Critical Review*; Environment Agency: Bristol, UK, 2003.
65. National Research Council; Division on Earth and Life Studies; Water Science and Technology Board; Committee on Bioavailability of Contaminants in Soils and Sediments. *Bioavailability of Contaminants in Soils and Sediments: Processes, Tools, and Applications*; The National Academies Press: Washington, DC, USA, 2003.
66. Ruby, M.V.; Davis, A.; Link, T.E.; School, R.; Chaney, R.L.; Freeman, G.B.; Bergstrom, P. Development of an in Vitro Screening Test To Evaluate the in Vivo Bioaccessibility of Ingested Mine-Waste Lead. *Environ. Sci. Technol* **1993**, *27*, 2870–2877. [CrossRef]
67. Li, J.; Li, K.; Cave, M.; Li, H.B.; Ma, L.Q. Lead bioaccessibility in 12 contaminated soils from China: Correlation to lead relative bioavailability and lead in different fractions. *J. Hazard. Mater.* **2015**, *295*, 55–62. [CrossRef] [PubMed]
68. Ollson, C.J.; Smith, E.; Scheckel, K.G.; Betts, A.R.; Juhasz, A.L. Assessment of arsenic speciation and bioaccessibility in mine-impacted materials. *J. Hazard. Mater.* **2016**, *313*, 130–137. [CrossRef]
69. Foulkes, M.; Millward, G.; Henderson, S.; Blake, W. Bioaccessibility of U, Th and Pb in solid wastes and soils from an abandoned uranium mine. *J. Environ. Radioact.* **2017**, *173*, 85–96. [CrossRef]
70. Rodrigues, S.M.; Cruz, N.; Carvalho, L.; Duarte, A.C.; Pereira, E.; Boim, A.G.F.; Alleoni, L.R.F.; Römkens, P.F.A.M. Evaluation of a single extraction test to estimate the human oral bioaccessibility of potentially toxic elements in soils: Towards more robust risk assessment. *Sci. Total Environ.* **2018**, *635*, 188–202. [CrossRef] [PubMed]
71. Ahmad, M.; Soo Lee, S.; Yang, J.E.; Ro, H.M.; Han Lee, Y.; Sik Ok, Y. Effects of soil dilution and amendments (mussel shell, cow bone, and biochar) on Pb availability and phytotoxicity in military shooting range soil. *Ecotoxicol. Environ. Saf.* **2012**, *79*, 225–231. [CrossRef] [PubMed]
72. Udovic, M.; McBride, M.B. Influence of compost addition on lead and arsenic bioavailability in reclaimed orchard soil assessed using Porcellio scaber bioaccumulation test. *J. Hazard. Mater.* **2012**, *205–206*, 144–149. [CrossRef] [PubMed]
73. Cai, M.; McBride, M.B.; Li, K. Bioaccessibility of Ba, Cu, Pb, and Zn in urban garden and orchard soils. *Environ. Pollut.* **2016**, *208*, 145–152. [CrossRef]
74. Brasil. *Manual de Métodos Analíticos Oficiais para Fertilizantes e Corretivos*; Ministério da Agricultura, Pecuária e Abastecimento (MAPA): Brasília, Brazil, 2017.
75. Empresa Brasileira de Pesquisa Agropecuária (EMBRAPA). *Manual de Métodos de Análise de Solo*, 2nd ed.; EMBRAPA: Rio de Janeiro, Brazil, 2017.
76. Kiehl, E.J. *Fertilizantes Orgânicos*; Editora Agronômica "Ceres" Ltd.: Piracicaba, Brazil, 1985.
77. Silva, F.C. *Manual de Análises Químicas de Solos, Plantas e Fertilizantes*; Empresa Brasileira de Pesquisa Agropecuária: Brasília, Brazil, 2009.
78. Alcarde, J.C. *Manual de Análise de Fertilizantes*; FEALQ: Piracicaba, Brazil, 2009.
79. American Society for Testing and Materials (ASTM). *D4646: Standard Test Method for 24-h Batch-Type Measurement of Contaminant Sorption by Soils and Sediments*; ASTM: West Conshohocken, PA, USA, 2016.
80. Raimondi, I.M.; Lima, J.Z.; Rodrigues, V.G.S. The Characterization of Tropical Peats for Potentially Toxic Metals Adsorption Purposes in an Abandoned Mine Area. In Proceedings of the IAEG/AEG Annual Meeting Proceedings, San Francisco, CA, USA, 17–21 September 2018; pp. 129–134. [CrossRef]
81. Lim, S.-F.; Lee, A.Y.W. Kinetic study on removal of heavy metal ions from aqueous solution by using soil. *Environ. Sci. Pollut. Res.* **2015**, *22*, 10144–10158. [CrossRef] [PubMed]
82. Wang, J.; Guo, X. Adsorption kinetic models: Physical meanings, applications, and solving methods. *J. Hazard. Mater.* **2020**, *390*, 122156. [CrossRef] [PubMed]
83. Ho, Y.S.; McKay, G. The sorption of lead(II) ions on peat. *Water Res.* **1999**, *33*, 578–584. [CrossRef]
84. Ho, Y.S.; McKay, G. Pseudo-second order model for sorption processes. *Process Biochem.* **1999**, *34*, 451–465. [CrossRef]
85. Ho, Y.S.; Wase', D.; Forster, C.F. Removal of lead ions from aqueous solution using sphagnum moss peat as adsorbent. *Water SA* **1996**. [CrossRef]

86. Ho, Y.S. Isotherms for the Sorption of Lead Onto Peat: Comparison of Linear and Non-Linear Methods. *Polish J. Environ. Stud.* **2006**, *15*, 81–86.
87. Ho, Y.S.; McKay, G. Sorption of dye from aqueous solution by peat. *Chem. Eng. J.* **1998**, *70*, 115–124. [CrossRef]
88. Azizian, S. Kinetic models of sorption: A theoretical analysis. *J. Colloid Interface Sci.* **2004**, *276*, 47–52. [CrossRef]
89. Inyang, H.I.; Onwawoma, A.; Bae, S. The Elovich equation as a predictor of lead and cadmium sorption rates on contaminant barrier minerals. *Soil Tillage Res.* **2016**, *155*, 124–132. [CrossRef]
90. Lee, S.Y.; Choi, H.J. Persimmon leaf bio-waste for adsorptive removal of heavy metals from aqueous solution. *J. Environ. Manag.* **2018**, *209*, 382–392. [CrossRef]
91. Rangabhashiyam, S.; Balasubramanian, P. Characteristics, performances, equilibrium and kinetic modeling aspects of heavy metal removal using algae. *Bioresour. Technol. Rep.* **2019**, *5*, 261–279. [CrossRef]
92. Sen Gupta, S.; Bhattacharyya, K.G. Kinetics of adsorption of metal ions on inorganic materials: A review. *Adv. Colloid Interface Sci.* **2011**, *162*, 39–58. [CrossRef] [PubMed]
93. Elovich, S.Y.; Larinov, O.G. Theory of adsorption from solutions of non electrolytes on solid (I) equation adsorption from solutions and the analysis of its simplest form, (II) verification of the equation of adsorption isotherm from solutions. *Izv. Akad. Nauk. SSSR Otd. Khim. Nauk.* **1962**, *2*, 209–216.
94. Mckay, G. The Adsorption of basic dye onto silica from aqueous solution-solid diffusion model. *Chem. Eng. Sci.* **1984**, *39*, 129–138. [CrossRef]
95. Mathews, A.P.; Weber, W. Effects of external mass transfer and intraparticle diffusion on adsorption rates in slurry reactors. *AIChE Symp. Ser.* **1977**, *73*, 91–98.
96. Weber, W.J.; Morris, J.C. Kinetics of adsorption on carbon from solution. *J. Sanit. Eng. Div.* **1963**, *89*, 31–60. [CrossRef]
97. Poggio, L.; Vrščaj, B.; Schulin, R.; Hepperle, E.; Ajmone Marsan, F. Metals pollution and human bioaccessibility of topsoils in Grugliasco (Italy). *Environ. Pollut.* **2009**, *157*, 680–689. [CrossRef]
98. Jorge Mendoza, C.; Tatiana Garrido, R.; Cristian Quilodrán, R.; Matías Segovia, C.; José Parada, A. Evaluation of the bioaccessible gastric and intestinal fractions of heavy metals in contaminated soils by means of a simple bioaccessibility extraction test. *Chemosphere* **2017**, *176*, 81–88. [CrossRef] [PubMed]
99. Valente, B.S.; Xavier, E.G.; Morselli, T.B.G.A.; Jahnke, D.S.; Brum, B.S., Jr.; Cabrera, B.R.; Moraes, P.O.; Lopes, D.C.N. Fatores que afetam o desenvolvimento da compostagem de resíduos orgânicos. *Arch. Zootec.* **2009**, *58*, 59–85. [CrossRef]
100. Instituto de Pesquisas Tecnológicas do Estado de São Paulo (IPT). *Estudo das Possibilidades de Aproveitamento de Turfa no Estado de São Paulo. Relatório 12.761*; IPT: São Paulo, Brazil, 1979.
101. Dick, D.P.; Novotny, E.H.; Dieckow, J.; Bayer, C. Química da matéria orgânica no solo. In *Química e Mineralogia do Solo*; Mello, J.W., Alleoni, L.R., Eds.; Sociedade Brasileira de Ciência do Solo: Viçosa, Brazil, 2009; pp. 1–68.
102. American Society for Testing and Materials (ASTM). *D4427: Standard Classification of Peat Samples by Laboratory Testing*; ASTM: West Conshohocken, PA, USA, 2013.
103. Sparks, D.L. *Environmental Soil Chemistry*; Elsevier: Amsterdam, The Netherlands, 1995.
104. Companhia Ambiental do Estado de São Paulo (CETESB). *Decisão de Diretoria 256/2016/E. Relatório de Estabelecimento de Valores Orientadores para Solos e Águas Subterrâneas no Estado de São Paulo*; CETESB: São Paulo, Brazil, 2016.
105. Venegas, A.; Rigol, A.; Vidal, M. Viability of organic wastes and biochars as amendments for the remediation of heavy metal-contaminated soils. *Chemosphere* **2015**, *119*, 190–198. [CrossRef]
106. Simantiraki, F.; Gidarakos, E. Comparative assessment of compost and zeolite utilisation for the simultaneous removal of BTEX, Cd and Zn from the aqueous phase: Batch and continuous flow study. *J. Environ. Manag.* **2015**, *159*, 218–226. [CrossRef] [PubMed]
107. Guermandi, J.I. Evaluation of Physical, Chemical and Microbiological Parameters of na Organic Fertilizer Produced by Composting and Vermicomposting of Organic Fraction of Municipal Solid Wastes Collected in São Carlos City. Master's Thesis, São Carlos School of Engineering (EESC), University of São Paulo (USP), São Carlos, Brazil, 2015.
108. Faverial, J.; Boval, M.; Sierra, J.; Sauvant, D. End-product quality of composts produced under tropical and temperate climates using different raw materials: A meta-analysis. *J. Environ. Manag.* **2016**, *183*, 909–916. [CrossRef]
109. Petroni, S.L.G. Kinetic and Equilibrium Evaluation of the Adsorption Process of Cadmium, Copper and Nickel Metal Ions in Peat. Ph.D. Thesis, Nuclear and Energy Research Institute (IPEN), Associated to the University of São Paulo (USP), São Paulo, Brasil, 2004.
110. Gündoğan, R.; Acemioğlu, B.; Alma, M.H. Copper (II) adsorption from aqueous solution by herbaceous peat. *J. Colloid Interface Sci.* **2004**, *269*, 303–309. [CrossRef]
111. Batista, A.P.S.; Romão, L.P.C.; Arguelho, M.L.P.M.; Garcia, C.A.B.; Alves, J.P.H.; Passos, E.A.; Rosa, A.H. Biosorption of Cr(III) using in natura and chemically treated tropical peats. *J. Hazard. Mater.* **2009**, *163*, 517–523. [CrossRef]
112. Swift, R.S. Organic Matter Characterization. In *Methods of Soil Analysis: Part 3 Chemical Methods*; Soil Science Society of America: Madison, WI, USA, 1996; pp. 1011–1068.
113. Chwastowski, J.; Staroń, P.; Kołoczek, H.; Banach, M. Adsorption of hexavalent chromium from aqueous solutions using Canadian peat and coconut fiber. *J. Mol. Liq.* **2017**, *248*, 981–989. [CrossRef]
114. Soobhany, N.; Gunasee, S.; Rago, Y.P.; Joyram, H.; Raghoo, P.; Mohee, R.; Garg, V.K. Spectroscopic, thermogravimetric and structural characterization analyses for comparing Municipal Solid Waste composts and vermicomposts stability and maturity. *Bioresour. Technol.* **2017**, *236*, 11–19. [CrossRef] [PubMed]

115. Liu, L.; Wang, S.; Guo, X.; Wang, H. Comparison of the effects of different maturity composts on soil nutrient, plant growth and heavy metal mobility in the contaminated soil. *J. Environ. Manag.* **2019**, *250*, 109525. [CrossRef]
116. International Union of Pure and Applied Chemistry (IUPAC). Reporting Physisorption Data for Gas/Solid Systems with Special Reference to the Determination of Surface Area and Porosity. *Pure Appl. Chem.* **1982**, *54*, 2201–2218. [CrossRef]
117. Franchi, J.G. The Utilization of Peat as Heavy Metal Adsorbent. The Example of the Contamination of Ribeira do Iguape River Catchment by Lead and Associated Minerals. Ph.D. Thesis, University of São Paulo (USP), São Paulo, Brazil, 2004.
118. Qin, F.; Wen, B.; Shan, X.Q.; Xie, Y.N.; Liu, T.; Zhang, S.Z.; Khan, S.U. Mechanisms of competitive adsorption of Pb, Cu, and Cd on peat. *Environ. Pollut.* **2006**, *144*, 669–680. [CrossRef]
119. Bartczak, P.; Norman, M.; Klapiszewski, Ł.; Karwańska, N.; Kawalec, M.; Baczyńska, M.; Wysokowski, M.; Zdarta, J.; Ciesielczyk, F.; Jesionowski, T. Removal of nickel(II) and lead(II) ions from aqueous solution using peat as a low-cost adsorbent: A kinetic and equilibrium study. *Arab. J. Chem.* **2018**, *11*, 1209–1222. [CrossRef]
120. Sharma, D.C.; Forster, C.F. Removal of Hexavalent Chromium Using Sphagnum Moss Peat. *Water Res.* **1993**, *27*, 1201–1208. [CrossRef]
121. Schiewer, S.; Volesky, B. Modeling multi-metal ion exchange in biosorption. *Environ. Sci. Technol.* **1996**, *30*, 2921–2927. [CrossRef]
122. Ho, Y.S. *Adsorption of Heavy Metals from Waste Streams by Peat*; School of Chemical Engineering, Faculty of Engineering, University of Birmingham: Birmingham, UK, 1995.
123. Gosset, T.; Trancart, J.L.; Thévenot, D.R. Batch Metal Removal by Peat—Kinetics and Thermodynamics. *Water Res.* **1986**, *20*, 21–26. [CrossRef]
124. Brookins, D.G. *Eh-pH Diagrams for Geochemistry*; Springer Science & Business Media: New York, NY, USA, 2012.
125. Ong, H.L.; Swanson, V.E. Adsorption of copper by peat, lignite, and bituminous coal. *Econ. Geol.* **1966**, *61*, 1214–1231. [CrossRef]
126. McKay, G.; Porter, J.F. Equilibrium Parameters for the Sorption of Copper, Cadmium and Zinc Ions onto Peat. *J. Chem. Tech. Biotechnol.* **1997**, *69*, 309–320. [CrossRef]
127. Alleoni, L.R.; Mello, J.W.V.; Rocha, W.S.D. Eletroquímica, adsorção e troca iônica no solo. In *Química e Mineralogia do Solo*; Mello, J.W., Alleoni, L.R., Eds.; Brazilian Soil Science Society: Viçosa, Brazil, 2009; pp. 69–130.
128. Pearson, R.G. Hard and soft acids and bases, HSAB, part I: Fundamental principles. *J. Chem. Educ.* **1968**, *45*, 581–587. [CrossRef]
129. McBride, M.B. *Environmental Chemistry of Soils*; Oxford University Press: New York, NY, USA, 1994.
130. Raimondi, I.M.; Vieira, E.M.; Vaz, L.A.A.; Rodrigues, V.G.S. Comparison of sugarcane pressmud with traditional low-cost materials. *Int. J. Environ. Sci. Technol.* **2021**, 1–18. [CrossRef]
131. Shah, G.M.; Imran, U.M.; Bakhat, H.F.; Hammad, H.M.; Ahmad, I.; Rabbani, F.; Khan, Z.U.H. Kinetics and equilibrium study of lead bio-sorption from contaminated water by compost and biogas residues. *Int. J. Environ. Sci. Technol.* **2019**, *16*, 3839–3850. [CrossRef]
132. Wang, B.; Gao, B.; Wan, Y. Comparative study of calcium alginate, ball-milled biochar, and their composites on aqueous methylene blue adsorption. *Environ. Sci. Pollut. Res.* **2019**, *26*, 11535–11541. [CrossRef]
133. Rizzuti, A.M.; Newkirk, C.R.; Wilson, K.A.; Cosme, L.W.; Cohen, A.D. Biosorption of hexavalent chromium from aqueous solutions using highly characterised peats. *Mires Peat* **2017**, *19*, 1–10. [CrossRef]
134. Wu, F.C.; Tseng, R.L.; Juang, R.S. Kinetic modeling of liquid-phase adsorption of reactive dyes and metal ions on chitosan. *Water Res.* **2001**, *35*, 613–618. [CrossRef]
135. Lima, J.Z.; Raimondi, I.M.; Rodrigues, V.G.S. Cd Adsorption by Chemically Activated Tropical Peat. In Proceedings of the Geotechnical Engineering in the XXI Century: Lessons Learned and Future Challenges, Cancun, Mexico, 17–20 November 2019; Lópes-Costa, N.P., Martínez-Hernánde, E., Espinosa-Santioago, A.L., Promotor, J.A., López, A.O., Eds.; IOS Press: Cancun, Mexico, 2019.